[American Journal of Science, Vol. 310, April, 2010, P. 231–260, DOI 10.2475/04.2010.01]

American Journal of Science

APRIL 2010

THE THERMOCHRONOLOGICAL RECORD OF TECTONIC AND SURFACE PROCESS INTERACTION AT THE YAKUTAT–NORTH AMERICAN COLLISION ZONE IN SOUTHEAST ALASKA

E. ENKELMANN*, P. K. ZEITLER**, J. I. GARVER***, T. L. PAVLIS[§], and B. P. HOOKS[§]

ABSTRACT. We investigate the material fluxes in space and time as a result of exhumation and erosion processes at the ongoing Yakutat–North American collision in southeast Alaska. Many thermochronologic studies using a variety of sampling strategies are challenged by the widespread ice cover that limit field observations and accessibility. This paper reviews new and published low-temperature thermochronological data from southeast Alaska to give a comprehensive interpretation of the exhumation patterns through time and how they are influenced by surface processes and climate change. We find that the southeastern margin of Alaska was exhumed and eroded long before the late Miocene–Pliocene Yakutat collision, but since the beginning of the subduction of the Yakutat lithosphere in the Oligocene/early Miocene. Today there is a distinct pattern of exhumation in southeast Alaska with a localized very rapid and deep-seated exhumation at the Yakutat plate corner (St. Elias syntaxis), where strike slip motion changes to convergence. Exhumation is also rapid, but less deep along the dextral Fairweather fault, and in the evolving fold and thrust belt. We present a re-interpretation of the exhumation pattern in the fold and thrust belt and suggest that mass transport by exhumation is parallel to the observed active thrust faults and oblique to the suture zone and orogenic strike. The locus of most rapid exhumation migrated from northwest to southeast with Recent exhumation occurring near the St. Elias syntaxis. Exhumation of the Chugach terrane rocks is still active, however to a lesser degree than on the south side of the orogen where precipitation rates are much higher. The Wrangellia terrane to the north has experienced little exhumation and has essentially formed the backstop for terrane accretion in southeast Alaska since the Early Cretaceous. Apatite U-Th/He ages give the first evidence that rocks of the Wrangell Range have only been recently uplifted and eroded as a consequence of the continuing Yakutat collision. In general the thermochronology in southeast Alaska reveals that climate variations across the region as well as changes through time have a limited influence on the pattern of erosion and that the location of deep exhumation is primarily influenced by tectonic processes.

Key words: Thermochronology, Alaska, Exhumation, Active tectonic, (U-Th)/He, Fission track, St. Elias.

* Institut für Geowissenschaften, Universität Tübingen, Wilhelmstrasse 56, 72074 Tübingen, Germany, phone: +49 7071 2973151; eva.enkelmann@uni-tuebingen.de

** Earth and Environmental Science, Lehigh University, 31 Williams Drive, Bethlehem, Pennsylvania 18015, phone: 610-758-3688/3671; peter.zeitler@lehigh.edu

*** Department of Geology, Union College, 807 Union Street, Schenectady, New York 12308-2311, phone: 518-388-6517; garverj@union.edu

§ Department of Geological Sciences, University of Texas at El Paso, 500 West University Boulevard, El Paso, Texas 79968, phone: 915-747-5570; pavlis@geo.utep.edu, bphooks@utep.edu

INTRODUCTION

The subduction–collision of the Yakutat terrane with North America has shaped the geologic and topographic evolution in southern Alaska since the Oligocene. The ongoing collision of the Yakutat terrane started in the late Miocene and has since formed the Earth's highest coastal mountain range, the Chugach–St. Elias, in southeast Alaska. The geodynamics of this active collision zone is characterized by the indenting lithospheric corner of the Yakutat terrane, where strike-slip motion transitions into convergence. This region is seismically active and extensively glaciated, making the Chugach–St. Elias Range a natural example to study the interplay between surface processes and active tectonics.

Because of the way the thermochronometric record integrates the material flux over time and space, it is a useful tool for studying erosion and exhumation processes (for example Batt and others, 2001; Batt and Brandon, 2002; Lock and Willet, 2008). Numerous thermochronometric studies have been performed in southeast Alaska using a variety of sampling strategies, many of them challenged by the ice coverage of the region that limits field observations and accessibility (for example O'Sullivan and others, 1997; Spotila and others, 2004; Meigs and others, 2008; Berger and others, 2008a; Berger and Spotila, 2008; Enkelmann and others, 2008, 2009). This paper reviews new and published low-temperature thermochronological data from southeast Alaska to give a comprehensive interpretation of the exhumation patterns through time, and how they are influenced by surface processes and tectonics. We find that the southeastern margin of Alaska was exhumed and eroded long before the late Miocene–Pliocene Yakutat collision, but since the beginning of the Yakutat lithosphere subduction in the Oligocene. We find large variations in erosional material flux across the orogen and along its strike. This variation is mainly controlled by tectonics and only secondarily appears to be related to the Late Miocene to Recent pattern of snow, ice and precipitation. Even though glacial erosion appears to be the prevalent means of erosion in the region, we recognize large variations in the efficiency of glacial erosion that depend strongly on crustal material flux provided by active faulting, requiring a change in our assumptions about glacial dynamics and subglacial hydrology.

BACKGROUND

Tectonics and Surface Process Interaction

Unlike oceanic lithosphere, plate boundary processes within continental lithosphere produce broad and diffuse zones of deformation heterogeneously distributed in space and time. Conceptual and numerical models have shown that the evolution of continental deformation zones is influenced by surface processes that shape landforms and redistribute mass. Surface processes can have fundamental effects on the geodynamics of mountain belts, and can influence the position of deformational fronts, initiate and localize faults, and cause crustal flow (for example Koons, 1987, 1990; Beaumont and others, 1992; Willet and others, 1993; Koons and others, 2002). Most studies that integrate surface process and tectonic activity consider fluvial erosion (for example Zeitler and others, 2001; Whipple and Meade, 2006), however, the importance of glacial erosion has been recognized due to the higher efficiency, and due to the widespread occurrence of extensive glaciations since the Plio- and Pleistocene (for example Raymo, 1994; Hallet and others, 1996; Meigs and Sauber, 2000; Tomkin and Braun, 2002; Tomkin and Roe, 2007). Many active orogens have undergone extensive glaciation in the past (Himalaya, Andes, European Alps), but today retain only small glaciers and remnant ice fields at high-elevation areas. Consequently, the geological and geomorphic observations we make in these areas mainly result from glacial erosion processes and their interaction with tectonics. Our understanding of how glaciers and tectonics interact is based on the geomorphic studies of remnant landscapes (Brockle-

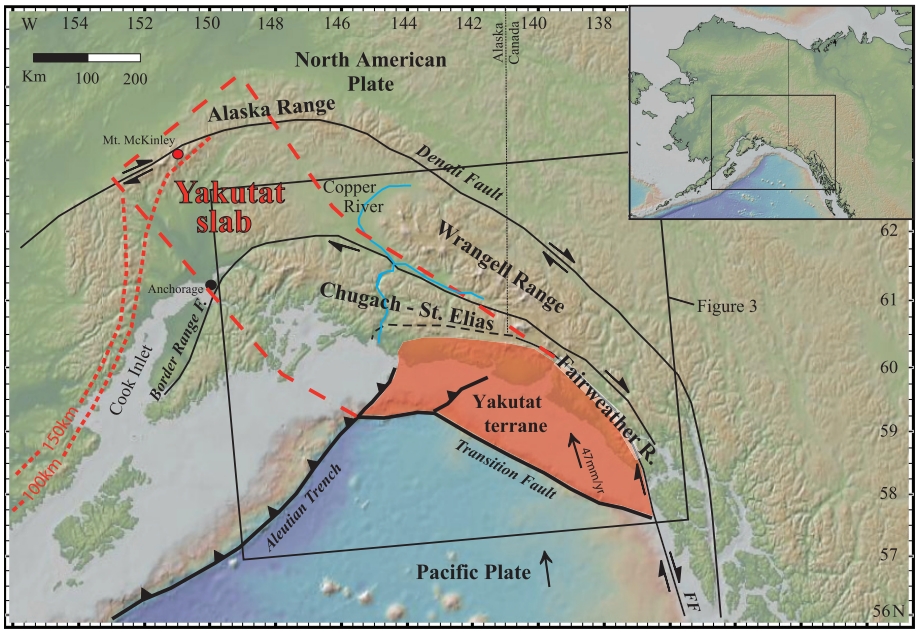

Fig. 1. General tectonic setting of southern Alaska with major tectonic structures and geographic features. Red dashed line indicates the extend of the subducted Yakutat flat slab (Zweck and others, 2002; Eberhart-Phillips and others, 2006; Fuis and others, 2008), red pointed line is the Pacific plate depths. Yakutat–North America plate motion vector from GPS measurements of Fletcher and Freymueller (2003). FF is the Fairweather fault.

hurst and Whipple, 2002, 2007), and on conceptual (Whipple and others, 1999), analytical (Tomkin and Roe, 2007), and numerical models (Tomkin and Braun, 2002; Tomkin, 2007). However, direct field observations providing information how glacial processes work in tectonically active areas are lacking. Southeast Alaska can be taken as the natural laboratory to study ongoing glacial erosion and tectonic interaction, whereby thermochronology can provide useful data to trace such processes.

Tectonic Setting and Context

Southern Alaska is characterized by the ongoing subduction–collision of the Yakutat terrane with North America (fig. 1). The Yakutat terrane was transported northward along the continental margin of North America by the dextral Queen Charlotte–Fairweather fault system, which initiated ca. 30 Ma (Plafker and others, 1978; Plafker, 1987). Today, the geology of southern Alaska is mainly a result of the Yakutat flat-slab subduction, whereas southeastern Alaska and parts of Canada are dominated by effects of the Yakutat collision (fig. 1). Recent geophysical studies imaged the entire Yakutat microplate as a 11 to 22 km thick low-velocity zone with a high ratio of P-wave to S-wave velocities, and characterized it as buoyant over thickened oceanic crust (Ferris and others, 2003; Eberhart-Phillips and others, 2006; Lowe and others, 2008; Christeson and others, 2008). The Yakutat terrane is separated from the Pacific plate by the Transition zone, and from the North American continent by the Aleutian megathrust in the west, the Chugach St. Elias thrust fault in the north, and the Fairweather transform in the east (fig. 1).

The Yakutat subduction–collision in southeast Alaska formed three mountain belts: the Chugach–St. Elias Range, the Fairweather Range, and the Wrangell Moun-

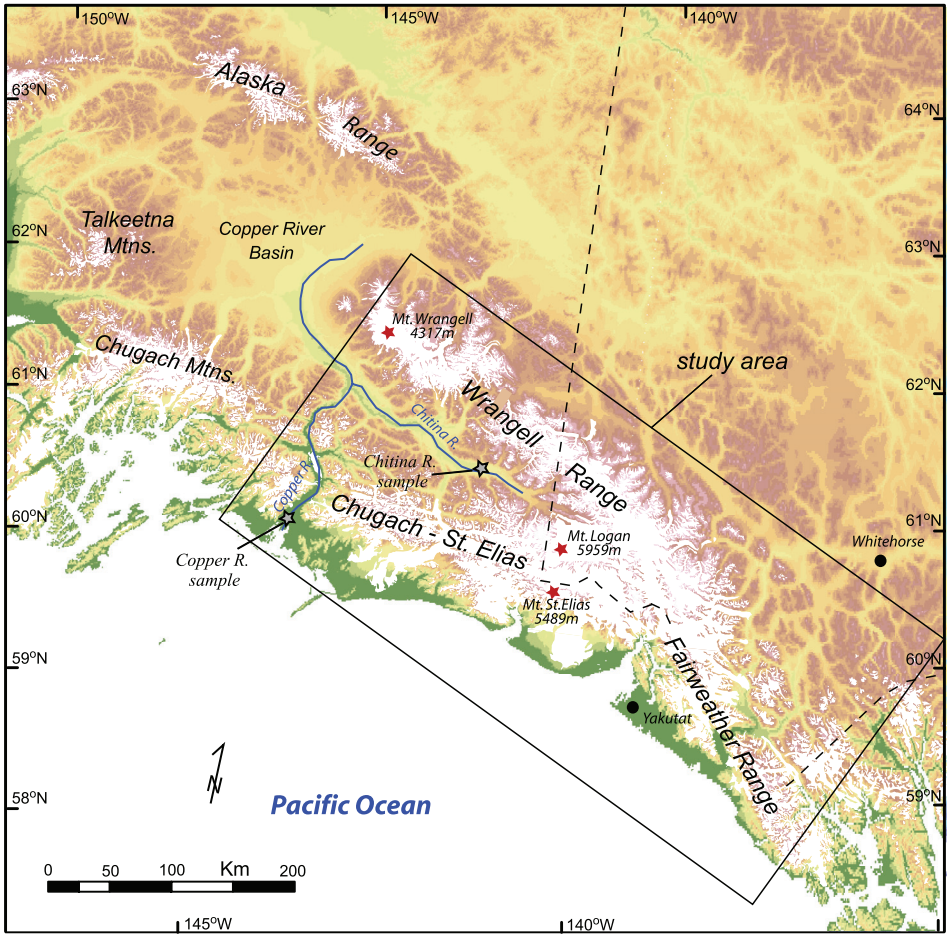

Fig. 2. Topographic map with ice coverage of southeast Alaska, highlighting main topographic features and the study area. Gray star: new detrital sample location of this study.

tains (fig. 2). Due to their high northern latitude (>58°N), high topography (peak elevations >5000 m), and proximity to the Pacific Ocean, the region receives annual precipitation of up to 7 m/yr and is extensively snow and ice covered (fig. 2). The three mountain ranges join together at the St. Elias syntaxis, the broad area of deflection of the structural and tectonic trends, to form the region of the highest peaks (Mt. Logan and Mt. St. Elias), highest mean elevation (>2500 m), and high local relief (>4000 m; fig. 2). The St. Elias syntaxis is the structural expression of crustal deformation manifested above the corner in the Yakutat lithoshere-scale plate where strike-slip motion changes to convergence (figs. 1 and 3; Hooks and others, 2009; Koons and others, 2010).

The Himalaya–Tibet system has been taken as type example to study geodynamic processes at continental collision zones, and in particular at plate corner settings. Numerical modeling, geophysical, and geological data from the eastern and western Himalayan syntaxis have shown that deep-seated crustal flow and strain localization occurs and is strongly coupled with erosion (for example Zeitler and others, 2001; Koons and others, 2002; Stewart and others, 2008; Booth and others, 2009). A positive

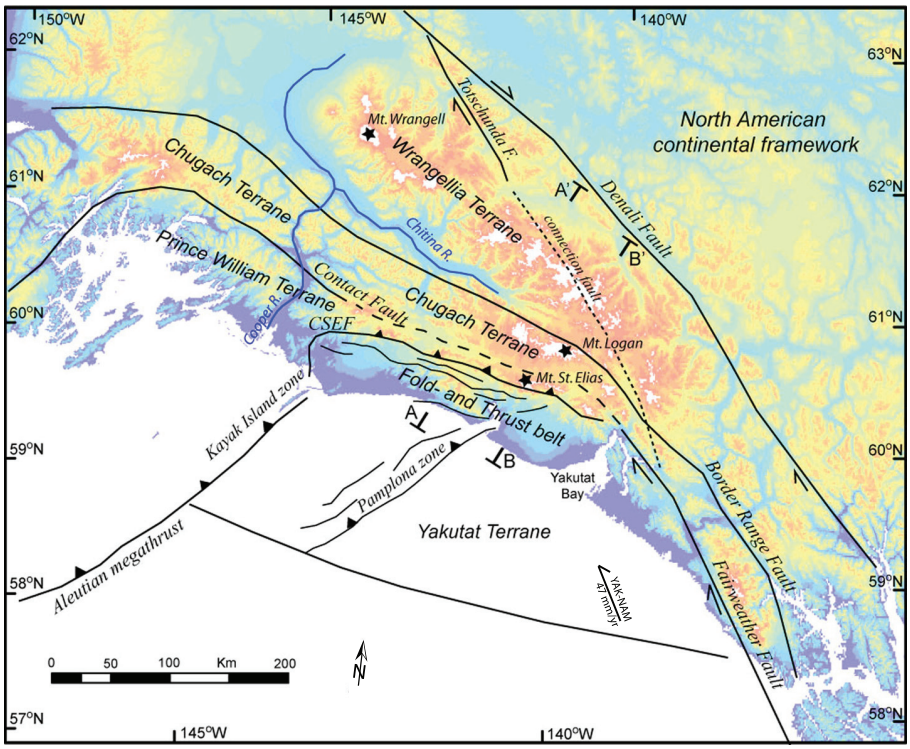

Fig. 3. Topographic map of southeast Alaska showing the main geological terranes and structures. CSEF: Chugach St. Elias Fault, which separates the Yakutat terrane from the Prince William terrane. The Border Range fault separates the Chugach terrane from either Alexander or Wrangellia terrane that form together the Wrangellia composite terrane. AA′ and BB′ indicate the location of the profiles shown in figure 5.

feedback develops between erosion and tectonics that produces localized crustal weakening due to advection of hot material to the surface, where it is efficiently evacuated by rivers. Over time this process builds up high mountain massifs with extreme local relief. This amplifying positive feedback mechanism has been described as a tectonic "aneurysm" (Zeitler and others, 2001; Koons and others, 2002). Similar coupling between intense erosion, localized crustal flow, and active faulting is inferred to occur at the St. Elias syntaxis (Enkelmann and others, 2009). As such we suspect that southeast Alaska can be taken as a type example of the "early" stage of this geodynamic setting. This early stage is overprinted, and largely obliterated, in orogens like the Himalayas or the European Alps and thus, southeast Alaska represents an important comparison to these older, more mature systems.

Geology of Southeast Alaska

In general, southern Alaska comprises a complex mosaic of terranes that have been accreted to North America since the Mesozoic. From north to south these terranes are: the Wrangellia Composite terrane, the Chugach/Prince William terrane, and the Yakutat terrane (fig. 3).

North of the Border Range fault (fig. 3), the Wrangellia composite terrane comprises late Paleozoic to Jurassic crystalline basement variably overlain by a cover sequence of Jurassic-Cretaceous forearc basin strata (Trop and others, 2002). The Wrangellia composite terrane was accreted to North America in mid Cretaceous time

(Trop and Ridgway, 2007), but its trailing edge, now exposed in the Chugach–St. Elias Mountains, was subjected to a north-directed thrusting event in Early Cretaceous (~145-130 Ma) time (Trop and others, 2002). Mid to Upper Cretaceous forearc basin strata and even younger, volcanic and plutonic rocks of the late Miocene to Recent Wrangell magmatic arc overlie latest Jurassic and older strata (MacKevett, 1978; Hudson, 1983; Nokleberg and others, 1994; Trop and others, 2002).

The Border Range fault is the suture between the Wrangellia Composite terrane and the Chugach terrane in the south (Pavlis and Roeske, 2007). The Chugach and Prince William terrane represent a Mesozoic-Paleogene subduction accretionary complex that was metamorphosed and intruded by the Sanak–Baranof plutonic belt during Eocene ridge subduction forming the Chugach metamorphic complex (Plafker and others, 1977, 1994; Barker and others, 1992; Cowan, 2003; Sisson and others, 2003; Pavlis and others, 2003). The Border Range fault was reactivated as a major dextral strike-slip fault during Paleogene ridge-trench interactions and accumulated at least 130 km of offset prior to ~50 Ma and total Late Cretaceous to Eocene offset could be 600 km or more (Pavlis and Roeske, 2007).

The Chugach terrane is separated from the Prince William terrane by the Contact fault. Although the Contact fault is thought to have initiated as a subduction thrust (Plafker and others, 1994), it is inferred to have been reactivated as the western continuation of the dextral Fairweather transform fault during Yakutat collision (Bruhn and others, 2004). The thickened crust of the Yakutat terrane is inferred to have arrived at the Aleutian subduction zone at ~10 to 5 Ma and has since been progressively colliding (Plafker and others 1994). With this collision, the Tertiary sedimentary cover of the Yakutat terrane has been scraped off basement rocks and has been accreted to North America in the evolving fold and thrust belt (fig. 3).

The Yakutat sedimentary cover comprises three units that show little or no evidence of metamorphism but show major thickness variations across the Yakutat terrane from near zero in the east to more than 10 km offshore (Plafker, 1987; Meigs and others, 2008; Gulick and others, 2009). Sedimentary thickness variations are closely associated with changes in basement across the Yakutat terrane, with accretionary complex rocks of the Yakutat Group to the east and an oceanic basement to the west (Plafker and others, 1994). The boundary between these two basement types is the Dangerous River zone (Plafker, 1987), and the western basement is now known to be a thickened oceanic basement that probably represents an oceanic plateau (Christeson and others, 2008). These basement distinctions are important to this study because basement massifs have been uplifted and exhumed in the St. Elias syntaxis region, but are absent west of Mount St. Elias. The imbricated Yakutat cover rocks include lower Eocene–Oligocene Kultieth Fm., the upper Eocene–upper Miocene Poul Creek Fm., and the synorogenic fluvial, and glacial marine upper Miocene–Pleistocene Yakataga Fm. that was deposited in response to orogenic growth since ~6 to 5 Ma (Plafker, 1987; Lagoe and others 1993; Plafker and others, 1994).

Glacial System of Southeast Alaska

Many glaciers and ice fields with hundreds of meters of ice thickness cover the mountain ranges of southeast Alaska. The Bagley Ice field–Seward Glacier system comprises one of the largest masses of temperate ice on the planet and mantles the top of the Chugach–St. Elias orogenic spine (figs. 2 and 4). This ice field is ca. 200 km long and 10 km wide, and the Bering and the Malaspina Glacier form the two main outlets that allow the southward evacuation of sediments into the Pacific Ocean (fig. 4). To the north the Bagley Ice field–Seward Glacier system is connected with numerous other ice fields and glaciers that drain northward into the Chitina River where sediments are transported west and eventually into the Pacific Ocean through the Copper River (fig. 2). Glaciers dominate the area today but they have been much more extensive during

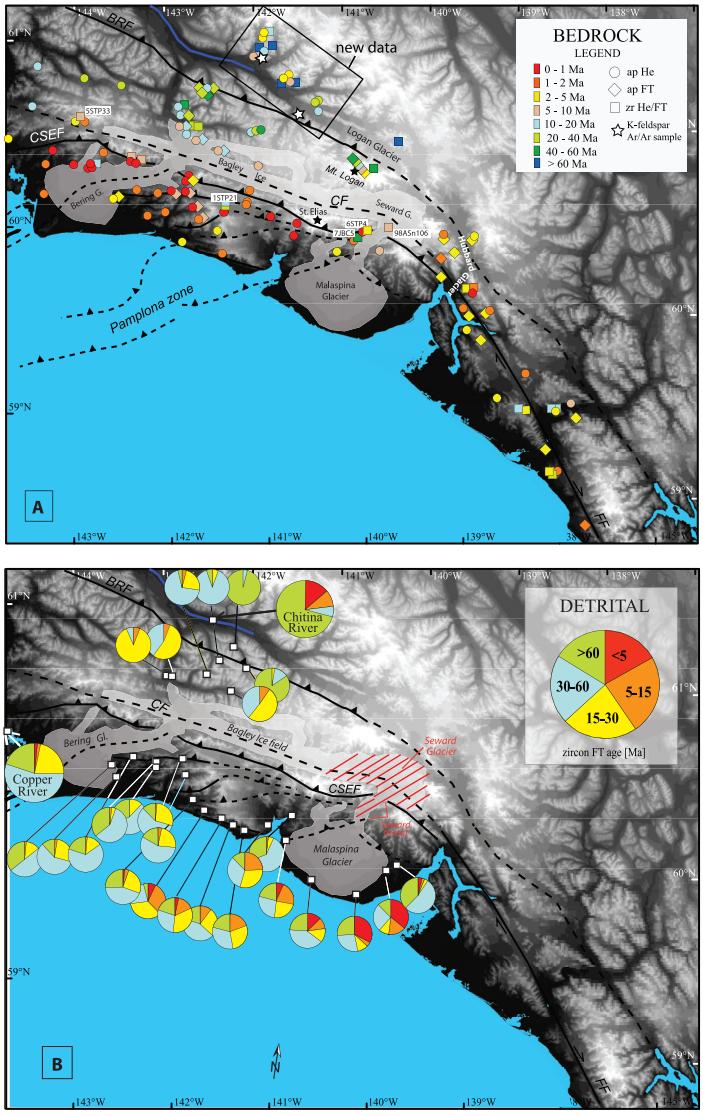

Fig. 4. Overview of all apatite and zircon thermochronometric ages in the study area. (A) Overview of bedrock apatite and zircon U-Th/He and FT ages of O'Sullivan and Currie, 1996; O'Sullivan and others, 1997; Spotila and others, 2004; Berger and others, 2008a; Berger and Spotila, 2008; Meigs and others, 2008; McAleer and others, 2009, and this study. (B) Overview of detrital zircon FT analysis on modern river sand deposits. Single grain ages are presented in age groups with increasing size. Data are from Enkelmann and others, 2008, 2009, and this study (Chitina and Copper River sample). Red lines indicate inferred source area of the youngest zircon FT ages from exhumed rocks (<3 Ma).

the entire Quaternary and before. During the last glacial maximum and similar periods of maximum glaciation the ice cover was much thicker than today and extended over much of the continental shelf. Glaciers in southeast Alaska were also sufficiently massive to reach the ocean and to shed debris-laden icebergs over 5 Ma, during a period that was generally warmer than today (Péwe, 1975; Lagoe and others, 1993; Lagoe and Zellers, 1996). Thus the beginning of glaciation in southeast Alaska can be set at the late Miocene/Pliocene boundary.

The patterns and rates of glacial erosions are likely to have changed through glacial-interglacial cycles and as the Yakutat collision has proceeded. The drainage basins as well as the locations where the ice funnels and slices through the mountain range probably changed through time as it is indicated by the different appearance of the two main southern outlet Glaciers. The ca. 15 km wide Bering Glacier coincides with the eastward extension of the Kajak Island zone that is the former location of the megathrust, and probably represents an older drainage than the only ca. 5 km wide Seward throat that connects the Seward Glacier with the Malaspina Glacier (fig. 3; Plafker and others, 1994). The Seward-Malaspina Glacier coincides with the onland extension of the Pamplona zone, which is the current deformational front of the megathrust (Plafker and others, 1994; Bruhn and others, 2004; Elliot and others, 2008), and is characterized by extremely rapid ice flow of up to 1600 m/yr (Headley and others, 2007).

Active Tectonics in Southeast Alaska

The Chugach–St. Elias and Fairweather ranges have been studied to understand the geodynamic processes and their interaction with erosion (for example Spotila and others, 2004; McAleer and others, 2009), but less is known about the Wrangell Mountains. The region along the southeastern Alaska coast, where the Yakutat terrane collides with North America, is characterized by high velocity plate motion vectors and high convergence rates of the Yakutat microplate with respect to stable North America (for example Fletcher and Freymueller, 1999, 2003; Freymueller and others, 2008). GPS measurements show that the 47 mm/yr convergence of the Yakutat terrane is quickly taken up by the Chugach–St. Elias fold and thrust belt and along the Fairweather fault, and that there is negligible motion across old inboard suture zones that separate the Prince William, Chugach, and Wrangellia terranes (for example Freymueller and others, 2008).

The Yakutat convergence coincides with high seismic activity dominated by reverse and strike-slip motion along the Alaskan coast and in near-coast areas (for example Ruppert, 2008). A number of >7.5 M earthquakes have been recorded from the Fairweather and St. Elias Range during the last century that caused several meters of uplift over tens of kilometers of shoreline (for example Plafker and Thatcher, 2008). In contrast, the regions farther north, and in particular the Wrangell Mountains, appear to be tectonically much less active. Westward motion of the entire southern Alaska block by counterclockwise rotation is accommodated by dextral strike-slip along the Denali fault, located north of the Wrangell Mountains (figs. 1 and 3; St. Armand, 1957; Lahr and Plafker, 1980). However, it has been suggested that a fault system exists under the ice cover that connects the Fairweather with the Denali fault through its active southern splay of the Totschunda fault (here postulated as "connection fault" on fig. 3; St. Amand, 1957; Richter and Matson, 1971; Kalbas and others, 2008).

Numerical models of the Pacific–Yakutat plate convergence with North America support this likely northward transfer of lateral strain from the Fairweather fault region (Koons and others, 2010). The model predicts development of an uplifted area that connects the Alaska Range and the Chugach–St. Elias Range as a lateral boundary, which coincides in its position with the Wrangell Mountains (Koons and others, 2010). This model suggests that the high topographic expression of the Wrangell Mountains is due to Miocene to Recent arc volcanism, as well as uplift that is a consequence of the Yakutat–North American subduction–collision.

OBSERVATIONS: THERMOCHRONOLOGY IN SOUTHEAST ALASKA

Low-temperature thermochronology provides time–temperature constraints on the cooling history of rocks in the upper crust, which can be related to geologic, tectonic, and erosional processes. Several thermochronometric studies have been

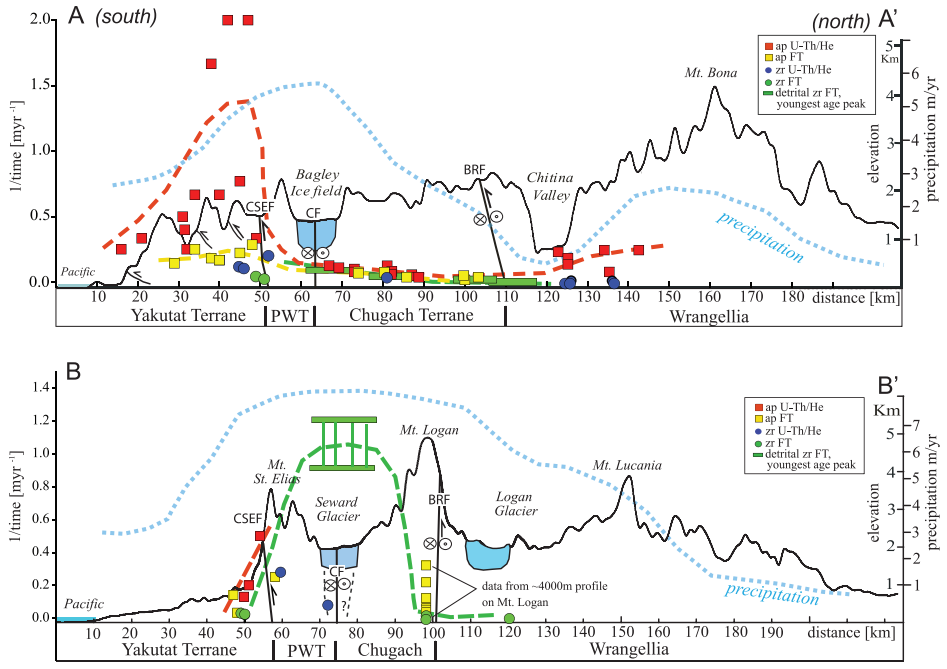

Fig. 5. Summary of all bedrock and detrital cooling ages along N-S profiles through the central Chugach–St. Elias orogen and perpendicular to the orogenic strike and the main structures. A-A′ profile cuts through the central part of the fold and thrust belt and the Wrangell Range. B-B′ crosses through the highest peak elevations and the indenter corner of the orogen. Cooling ages are plotted as 1/t to emphasize differences in young ages, which would otherwise be obscured by the large dynamic range if plotted linearly. The dashed lines are drawn to highlight the general age trends that are displayed by the different thermochronologic systems along the profile. Profile locations shown in figure 3. CSEF: Chugach St. Elias Fault, CF: Contact Fault, BRF: Border Range Fault.

performed in southeast Alaska using a variety of methods that reveal both young and old exhumation, and exhumation from shallow and deep crustal levels. However, due to extensive glaciation of this region, many of these studies give a limited and/or misleading picture of the exhumation history of the orogen. In the following we combine all published data with our new results to provide an integrated picture of the general exhumation patterns in southeast Alaska. A list of all new and published low-temperature thermochronology data that are discussed here is provided in the supplemental data repository and summarized in figures 4 and 5.

For the discussion that follows it is important to review the thermal sensitivity of the different thermochronological methods and their approximate closure temperature (Tc), the temperature of the sample at the time given by its apparent age (Dodson, 1973). Fission tracks (FT) in apatite are sensitive to annealing at temperatures ranging from 65 to 120°C and are effectively accumulated at the closure temperature of 100 to 110°C, which depends mainly on the chemical composition and cooling rate (for example Green and others, 1986; Carlson and others, 1999). The closure temperature for the apatite U-Th/He method is generally assumed to be 55 to 65°C, but can be much lower (45°C) for young apatites with low radiation damage, and much higher (115°C) for old apatites with high radiation damage (Schuster and others, 2006). Additionally the U-Th/He closure temperature in apatite depends on grain size and cooling rate. The zircon U-Th/He and FT systems are sensitive to higher temperatures with closure temperatures ranging from 170 to 190°C and ~210 to

290°C, respectively (for example Brandon and others, 1998; Reiners and others, 2004). The zircon U-Th/He closure temperature also depends on grain size and cooling rate, whereas fission track annealing in zircon depends mainly on the amount of radiation damage and cooling rate. Zircon grains with very low radiation damage are more resistant to fission track annealing, and the closure temperature of those grains can be 300 to 350°C (Yamada and others, 1995; Tagami and others, 1998; Rahn and others, 2004). Generally, the closure temperatures need to be used carefully as the closure temperature concept assumes continuous cooling since the time given by the apparent age (Dodson, 1973), which is probably not the case for all samples.

Thermochronological Challenges

Southeast Alaska is extensively glaciated with large interconnected ice fields and glaciers of >1500 m thickness that extend into the Pacific Ocean (for example Headley and others, 2007; Conway and others, 2009). This ice coverage limits the collection of bedrock samples to mountain ridges that tower over the ice. This sampling limitation could lead to significant interpretational bias that overemphasizes the signal from high-elevation exposures. For example, low-elevation samples are usually expected to yield the youngest cooling ages, and the degree to which this is true or not is an important signal about whether relief is growing or lowering or the local topography is in steady state. To access this key record in rock that is underneath ice and inaccessible for direct sampling, detrital material from modern rivers that drain glaciers provides another means of sampling regional cooling ages below the ice (Enkelmann and others, 2008, 2009). In contrast to bedrock, which yields a single age that records the cooling history of this particular rock sample, about 100 single grains are dated for a detrital sample to assess the cooling history of the entire catchment area. While detrital sampling loses spatial resolution and precision on single grain ages, it does improve sampling coverage and thus provides a more synoptic view of a watershed.

A key outcome from the detrital-sample studies in southeast Alaska is that their exhumation patterns differ considerably from those of the bedrock-sample studies in the same area (compare figs. 4A and B). These differences between bedrock and detrital data are the result of two things:

First, the bedrock data are dominated by apatite cooling ages, but the detrital dataset consists entirely of zircon FT ages. The apatite systems are sensitive to perturbations of the low temperature isotherms (<150°C), which can be affected by topography and vertical and lateral rock exhumation (for example Mancktelow and Graseman, 1997). Higher temperature isotherms (>200°C) are generally not affected by topography but can be perturbed by strong heat advection due to tectonic processes and intense erosion (Mancktelow and Graseman, 1997). As a consequence, the apatite systems are able to record the young and/or shallow exhumation processes, whereas the zircon systems preserve the record of deeper exhumation events over a longer time, thus they may allow a view into the older exhumation history.

The second reason for the difference between the bedrock and detrital ages comes from the different sampling strategies. In a fluvial drainage, the age distribution of a detrital sample generally integrates the bedrock cooling ages in the entire drainage area. In a drainage system occupied by glaciers, the detrital material is mainly derived from the ice covered part of the drainage basin, mainly valley bottoms. The amount of material that originates from above the ice contributed by rock fall and landslides is generally small and is transported to the side moraines as the glacier flow is typically faster in the middle than at the sides of the glacier. Bedrock sampling in glaciated regions is mostly limited to the high-elevation part of the drainage areas, the mountain ridges above the ice. This unique situation, which is particularly pronounced in heavily glaciated southeast Alaska, causes a natural horizontal separation of the two sampling areas that leads to a biased interpretation. For example, if erosion rates are

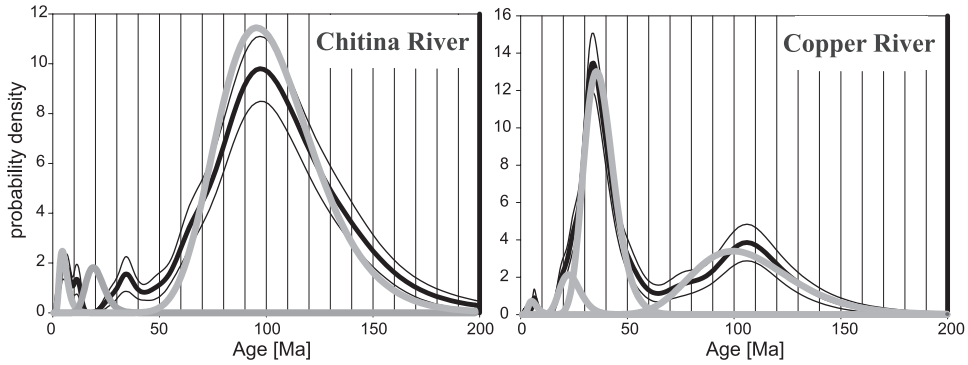

Fig. 6. Zircon FT age distribution (black) and the modeled age populations (gray) for the Chitina and Copper River samples, see table DR4 for details (http://earth.geology.yale.edu/~ajs/SupplementaryData/2010/04EnkelmannTableDR4.pdf).

different beneath glaciers compared to mountain ridges the landscape is not in steady state and relief will change through time.

New Thermochronological Data

We analyzed a set of bedrock samples from the eastern Wrangell Mountains (Alaskan territory) north of the Chitina Valley (fig. 3). Samples are from Early Permian and Pennsylvanian metasedimentary and magmatic rocks (Plakfer and others, 1989; Richter and others, 2006), and have been dated for apatite and zircon U-Th/He analysis and two granitic samples for K-feldspar $^{40}Ar/^{39}Ar$ analysis (see also fig. A1). We also dated five bedrock samples from the Chugach–St. Elias Range using zircon U-Th/He dating, and three of these samples have already been dated by the apatite U-Th/He method (Berger and others, 2008a; Berger and Spotila, 2008). Additionally, we analyzed detrital zircons from two river samples, one from the upper Chitina River and one from the Copper River Delta, using fission-track analysis (figs. 2, 4B, and 6). The main results are summarized here (table 1), and discussed together with published data below. Analytical details and data are reported in the supplemental data repository (table DR1, DR2, DR4 and DR5), http://earth.geology.yale.edu/~ajs/SupplementaryData/2010/01EnkelmannTableDR1.pdf; http://earth.geology.yale.edu/~ajs/SupplementaryData/2010/02EnkelmannTableDR2.pdf; http://earth.geology.yale.edu/~ajs/SupplementaryData/2010/04EnkelmannTableDR4.pdf; http://earth.geology.yale.edu/~ajs/SupplementaryData/2010/05EnkelmannTableDR5.pdf

Zircon U-Th/He cooling ages from the Wrangell Mountains are generally old (125-100 Ma; table 1) and reveal Early Cretaceous cooling of this part of Wrangellia. This finding is in agreement with the two K-feldspar $^{40}Ar/^{39}Ar$ analysis from the Late Jurassic Chitina batholith north of the Border Range fault, and a sample from the Pennsylvanian granitoid complex north of the Chitina Valley (fig. 4A) (Richter and others, 2006). For both samples, modeling of the K-feldspar temperature–time history reveals significant cooling from >350°C to 150°C at 140 to 125 Ma (fig. A1). This age range is significant regionally as this cooling period is coincident with the development of the Chitina valley thrust system and an associated angular unconformity in the Chitina Valley (for example Trop and others, 2002).

Apatite U-Th/He ages range from 24 to 4 Ma, with a distinct group of samples yielding cooling ages of 5 to 4 Ma [fig. 4A; tables 1 and supplemental data repository table 1 (http://earth.geology.yale.edu/~ajs/SupplementaryData/2010/01EnkelmannTableDR1.pdf)]. The zircon U-Th/He ages from the Chugach–St. Elias

TABLE 1

Summary of new apatite and zircon U-Th/He analysis

Sample	Latitude North	Longitude West	# of analysis	Mean apatite age [Ma]	Mean zircon age [Ma]
Chugach – St. Elias Mtns.			Zircon		
6STP4 quarzite, Orca Gr.	60° 14.128	140° 27.399	2	0.6 ± 0.1**	3.5 ± 0.7
7JBC05 metasiltstone, Yakutat Gr.	60° 13.320	140° 44.598	3	-	55 ± 5
6STP21 arcose, Poul Creek Fm.	60° 17.421	141° 57.543	2	0.7 ± 0.1*	38 and 18.5
5STP33 granite, Chugach terrane	60° 38.387	143° 43.260	2	1.7 ± 0.1**	8.8 ± 0.3
98ASn106 gneiss, Chugach terrane	60° 26.348	140° 16.156	2	-	9.6 ± 2
Wrangell Mtns.			Apatite /Zircon		
6EUT1 fine grained granite	61°15.753	141°52.045	3 / 2	4.5 ± 1	12.4 ± 3
6EUT2 monzonite granite (K-fsp)	61°11.207	141°47.679	5 / 3	12.1 ± 3	120 ± 17
6EUT3 monzonite granite	61°12.580	141°47.386	4 / 3	no mean	115 ± 36
6EUT4 monzonite granite	61°13.024	141°49.199	4 / 3	4.6 ± 1	125 ± 26
6EUT5 sedimentary-volcanic	61°08.188	141°56.582	4 / -	5.8 ± 1	
6EUT8 metapelite	61°01.009	141°32.360	- / 3		119 ± 45
6EUT9 breccia, metapelite	61°01.323	141°32.039	3 / -	8.0 ± 1	
6EUT10 fine monzonite granite	61°02.390	141°34.087	4 / 3	4.3 ± 1	100 ± 12
6EUT11 fine monzonite granite	61°02.782	141°33.802	4 / -	4.1 ± 1	
6EUT40 diorite	60°54.150	141°10.606	4 / -	9.9 ± 2	
6EUT41 diorite	60°56.746	141°11.683	3 / -	21.9 ± 2	
6EUT42 diorite	60°57.134	141°12.004	3 / -	24.0 ± 2	
6EUT35 granite (K-fsp)	60°52.203	141°14.236			

Note: Apatite analysis are multi-grain aliquots, zircon analysis are single grain aliquots. 1σ error. Data from *Berger and others, 2008a; **Berger and Spotila, 2008.

Range range from 3.5 to 55 Ma, whereby the oldest ages are from the Yakutat terrane basement and the cover strata, and the young cooling ages from the Chugach/Prince William terrane [table 1 and supplemental data repository table 2 (http://earth.geology.yale.edu/~ajs/SupplementaryData/2010/02EnkelmannTableDR2.pdf)]. The two detrital samples from modern river samples yielded quite different age populations (fig. 6); the Chitina River sample is dominated by zircon FT ages of >90 Ma and a very young age population of 4.5 Ma, while the Copper River sample is dominated by zircon FT ages of 20 to 40 Ma (fig. 4B; table 2).

TABLE 2

Detrital zircon fission track analysis

	Latitude	Longitude	N	Ma age range	P1	P2	P3	P4
Chitina R.	-142.464	61.12861	102	0.7 - 175	4.5 ± 0.4 [24]	19 ±1.4 [10]		95.6 ± 3.9 [66]
Copper R.	-145.074	60.44229	105	2 - 147	5.2 ± 0.7 [7]	22.4 ± 1.8 [11]	35.6 ± 1.4 [63]	99.6± 5.5 [19]

Note: N: number of single grains analyzed; P: best-fit age populations in Myr and 1σ error, calculated using BINOMFIT 1.1 (Brandon, 1996). The relative size of the age population in percent is given in brackets. Age range indicates the youngest and oldest single grain ages.

DISCUSSION

An important issue in the study of geodynamic processes is the interrelationship between tectonic, erosion, and climatic change on the evolution of active mountain ranges (for example Willet and others, 1993; Batt and Brandon, 2002; Whipple and Meade, 2006; Lock and Willet, 2008; Whipple, 2009). Thermochronology is a useful tool to trace the flux of material in the crust and reveals spatial variation in exhumation patterns and changes in exhumation through time. Reviewing all the thermochronology data of southeast Alaska provides an integrated view of the large-scale exhumation patterns in southeast Alaska and a comparison with observations in other orogens. Together these data allow a preliminary evaluation of glacial erosion models.

To summarize the regional thermochronology, we plotted topography, precipitation, and cooling ages as 1/time (which will scale roughly proportional to erosion rate) along two profiles normal to the strike of the St. Elias Range and the Wrangells and normal to the suture zones (figs. 3 and 5). From these profiles it can be seen that the region of the St. Elias syntaxis (Profile B-B′), and in particular the area of the Seward Glacier, has experienced the most intense rock exhumation from 5 to 10 km depth and cooling rates of >150 to 300°C/Myr (Enkelmann and others, 2009). This area of rapidly cooling rocks has <2 Ma zircon FT ages derived from the Malaspina Glacier deposits. Fission track and U/Pb double dating of the youngest FT age zircons revealed that these rapidly cooled rocks originate from the Chugach terrane and Yakutat basement. Chugach terrane rocks occur north of the Contact fault, located under the upper Seward Glacier, whereby the Yakutat basement rocks are located on the eastern Seward Glacier and under the Seward throat—the canyon of fast moving ice that connects the Seward with the Malaspina Glacier (fig. 4). None of the zircon U/Pb ages are <50 Ma and we did not find evidence for young zircon rims. Based on this result, plus the fact that there are no evidences for magmatic activity (for example hot springs or young magmatic dikes) we rule out a young magmatic source underneath the ice and interpret the FT ages as cooling ages due to rapid exhumation. The young age population of detrital zircons from the Chitina River suggests that the material from the syntaxis area is also transported to the north by the Logan Glacier (fig. 4B, table 2). The Hubbard Glacier connects with the ice covered region of the St. Elias syntaxis and transports sediments to the southeast, into Yakutat Bay. We hypothesize that those sediments carry comparable young cooling ages, but unfortunately they are transported and deposited into the Pacific Ocean and are not easily accessible. Due to the extensive ice-coverage it is unclear how the fast rock exhumation is structurally accommodated, but two alternatives are feasible which were both proposed based on thermochronological observations from the western part of the orogen, the Chugach–St. Elias range (north and south of the Bagley Ice field): [1] a back-thrust model as suggested by Berger and others (2008a) with a northward thrust (Bagley thrust) underneath the Bagley Ice field, or [2] a flower-structure model with rapidly exhuming slivers of crustal blocks along the reactivated Contact fault underneath the Bagley-Ice field Seward Glacier as suggested by Enkelmann and others (2008).

Rapid exhumation also occurs in two key areas in the orogen: along the Fairweather fault (fig. 4A), and in the fold and thrust belt of the Chugach–St. Elias Range (figs. 4 and 5A). Motion along the Fairweather fault is nearly pure strike-slip, but there is evidence for convergence and rock uplift, especially in high uplift rates measured by GPS (Larsen and others, 2004), a significant convergence from plate motion models (Pavlis and others, 2004), uplifted terraces associated with thrusting during the 1899 earthquake (Hudson and others, 1976; Plafker and Thatcher, 2008), numerical models revealing a high vertical velocity zone along the fault (Hooks, ms, 2009), rugged topography, and young cooling ages (O'Sullivan and others, 1997; McAleer and others, 2009). Thermochronology reveals young apatite cooling ages (5-1 Ma) on

both sides along the entire Fairweather fault that become older in samples farther away from the fault (fig. 4A; O'Sullivan and others, 1997; McAleer and others, 2009). Some Pliocene zircon U-Th/He and FT ages (4.5-2 Ma) occur in close proximity to the Fairweather fault and record local cooling from temperatures above ~180/250°C (McAleer and others, 2009).

Rapid erosion in the fold and thrust belt is evident by young apatite U-Th/He ages from the southern flanks of the Chugach–St. Elias Range (fig. 5A), the best studied part of southeast Alaska (fig. 4). Bedrock apatite ages are very young (4-0.5 Ma) at the south side of the mountain range and much older (40-8 Ma) on the north side (figs. 4A and 5A; Spotila and others, 2004; Berger and others, 2008a; Berger and Spotila, 2008; Meigs and others, 2008; Perry and others, 2009). This age distribution is broadly similar to the Recent precipitation pattern that shows extremely high rates of up to 7 m/yr occur at the south side of the orogen, whereas the area north of the Bagley Ice field is currently much dryer (~1 m/yr; fig. 5). The high precipitation and ongoing collision of the Yakutat terrane results in erosion, deposition, and reworking of cover strata during the development of the fold and thrust belt. Exhumation is rapid as indicated by apatite U-Th/He ages of <1 Ma (Berger and others, 2008a; Berger and Spotila, 2008). Zircon ages in the fold and thrust belt are generally old (>14 Ma) and show partial resetting or non-resetting. This is evident by the poor reproducibility of the single grain ages of individual samples with ages that are all older than the inferred exhumation event that brought them to the surface. The zircon ages thus provide a constraint on total exhumation. Specifically, rock exhumation in the fold and thrust belt does not bring material from great depth to the surface. The lateral transport of material into the fold and thrust belt, stripping of cover from basement in the thin-skinned thrust belt and subsequent exhumation affects only the upper 5 km of the crust and prevents exhumation from great depths (Meigs and others, 2008).

The dramatic contrast in bedrock cooling ages between the north and the south sides of the Chugach–St. Elias Range suggests that the Chugach terrane has acted as the deformation backstop for the Yakutat collision and the Contact fault has been reactivated as a back thrust (Berger and others, 2008a, 2008b; Berger and Spotila, 2008). New evidence does not support this hypothesis. Specifically, detrital zircon FT data reveal relatively young cooling ages (~10 Ma) from underneath the glaciers on the north side of the range, suggesting that exhumation rates are low at the mountain ridges above the glaciers, but in the valleys they are comparable to those at the south side. This discrepancy of bedrock cooling ages at the mountain ridges probably resembles the precipitation pattern that causes rapid erosion at the wet southern flanks and preservation of the dry northern flanks. The discrepancy between the old bedrock ages at the ridges and the young detrital ages from the valleys require a large vertical offset of sample ages. If this age change is gradual or sharp is unclear, however it can only be explained by strain gradients probably from localized faults like along the Contact fault. Generally, modern detrital zircon FT ages at the north side of the range become older towards the north (35 Ma) and are significantly older north of the Border Range fault within the Wrangellia terrane (>90 Ma; fig. 5; Enkelmann and others, 2008). A similar age pattern is shown by zircon FT ages and by the elevation discordance of apatite FT data reported from the Mt. Logan massif (O'Sullivan and Currie, 1996). Collectively these data, as well as the basic topographic form of the range, suggest that deformation has not been limited to the south side of the Chugach–St. Elias Range (fig. 5; Enkelmann and others, 2008). Thus, the Border Ranges fault and its hanging wall, the Wrangellia composite terrane, presumably formed the actual backstop for the bulk of the convergence history of the orogen.

Support for active deformation that is driving exhumation on the northern side of the Chugach–St. Elias Range comes from a numerical model of the Yakutat–North

American collision (Hooks, ms, 2009; Koons and others, 2010). A three-dimensional model of the mechanical–thermal evolution of southeast Alaska shows that the strike-slip strain of the Fairweather fault bifurcates at the Yakutat plate corner to form a two-sided orogenic wedge located northwest of the northern end of the Fairweather fault, forming the Chugach–St. Elias Range. This model orogenic wedge is characterized by a doubly-vergent thrust-fault system predicting active deformation not only on the south of the Chugach–St. Elias Range (within the fold and thrust belt) but also along the topographic northern flank of the range into the Chitina Valley (Hooks, ms, 2009).

Exhumation has been limited in the Wrangell Range, because the zircon cooling ages and K-feldspar modeling revealed that the last significant cooling event occurred in the Early Cretaceous (Appendix, fig. A1). Limited young exhumation of 1 to 3 km is indicated by the 5 to 4 Ma apatite U-Th/He ages (this study). Even so the Wrangell and the Chugach–St. Elias Range are similar in their topographic appearance and ice coverage, the difference in active rock exhumation between the two is obvious from the cooling ages (fig. 5A). This difference becomes evident in the two detrital samples collected from the upper Chitina River and the Copper River Delta (see location on figs. 2 and 4B). The drainage area of the upper Chitina River is mainly comprised of rock of Wrangellia and only partially of the Chugach terrane. Consequently it is not surprising that the sample is dominated (66%) by an Early Cretaceous zircon FT age typical for the Wrangellia terrane and only a small portion (11%) of the grains have cooling ages that are typical for the Chugach terrane (table 2). Interestingly, 24 percent of the sample is represented by a population of young (6-0.7 Ma) zircon FT ages that define a component population at 4 Ma. Given the nature of the drainage area it is likely that the source of this young population is the St. Elias syntaxis area. The Copper River sample reveals a different composition where the age signal of the upper Chitina River sample is much diluted. Nonetheless, the old ages of Wrangellia and the young age signatures of the syntaxis are well recorded, but their portions are reduced to 19 percent and 7 percent, respectively (table 2). The detrital signal is dominated by Eocene to Miocene zircon FT ages that are typical for the Chugach terrane. These ages compose 74 percent of the zircons in the Copper River Delta, emphasizing the dominant input of the northern flanks of the Chugach–St. Elias Range in contrast to the Wrangells (fig. 4).

The St. Elias Syntaxis

Localized intense exhumation at the St. Elias syntaxis is comparable to the observations in the Himalayan syntaxes where thermochronology revealed localized intense exhumation of mid-crustal rocks that causes the perturbation of the thermal structures (tectonic "aneurysm" model) in the areas of the Namche Barwa and Nanga Parbat massifs (Zeitler and others, 2001; Koons and others, 2002; Stewart and others, 2008). These regions of the Himalayan syntaxes are kinematically similar to the St. Elias syntaxis because in both regions the localized exhumation and deformation occur at the transition from strike-slip tectonics to convergence. The glacial cover in the Himalayas is less extensive than in southeast Alaska, but rivers efficiently erode and evacuate material out of the system. Reconstruction of lake sediments deposited in a glacially dammed lake along the Tsangpo River drainage at the eastern Himalayan syntaxis showed that the ELA during the last glacial maximum was up to 1000 m lower than today, located at 4100 to 4600 m elevation. In contrast, glaciers extended far on the continental shelf in southeast Alaska during the periods of glacial maximum in the Quaternary. Based on the investigations of the glacial lake sediments and modern and Holocene ELA in the eastern Himalayan syntaxis, Korup and Montgomery (2008) suggested that the damming of the Tsangpo River caused the intensification of erosion in the Tsangpo gorge and may have triggered the tectonic "aneurysm". The localized

perturbation of the isothermal structure in the Himalayan syntaxes has been mapped out by bedrock and detrital thermochronology in the region where the Indus River and the Brahmaputra River cut through the high massifs of the Nanga Parbat and Namche Barwa, respectively (for example Zeitler and others, 2001; Stewart and others, 2008; Booth and others, 2009). Apatite and zircon U-Th/He and FT ages are less than 2 Ma and the exhumation is intense enough to expose even higher temperature systems like biotite $^{40}Ar/^{39}Ar$ cooling ages of <3 Ma (Zeitler and others, 2001; Finnegan and others, 2008). Exhumation at the Himalayan syntaxis causes partial melting evident in <10 Ma sphene U/Pb and monazite U/Pb and Th/Pb ages (Zeitler and others, 2001; Booth and others, 2009). Zircon FT analysis from modern Brahmaputra River sediments has shown that 50 percent of the detrital zircons that are transported out of the Himalayan Range comes from only 2 percent of the drainage area, the area where the river cuts through the Namche Barwa massif (Stewart and others, 2008).

Sediments from the Malaspina Glacier yield a zircon FT age population at ~2 Ma that indicate that under the Seward Glacier is an area of deep-seated exhumation and rapid cooling from 300 to 350°C (Enkelmann and others, 2009). Similar to the Himalayan syntaxes, the proposed tectonic "aneurysm" in the St. Elias syntaxis coincides with the region of the highest mountain massifs and intense erosion that produces extreme local relief (>4000 m). In the St. Elias Range, however, bedrock thermochronology has failed so far to reveal the thermal perturbation of the tectonic "aneurysm" (fig. 4). However, it is important to point out that in the Himalayas sampling is usually conducted along valleys (lower elevation region), whereby in the St. Elias bedrock is only accessible on mountain ridges because the valleys are filled with ice. Thus the bedrock results are generally biased to high elevation rocks that are less affected by erosion than rocks under glaciers. The young zircon FT age population in the Chitina River sample (fig. 4B; this study) might suggest that the region of localized intense exhumation and isothermal perturbation extends north of the Seward Glacier. This northern region of the St. Elias syntaxis is covered by a complex system of ice fields and glaciers that interconnect and drain eventually westward into the Chitina River valley. The source of these young ages is probably very small in comparison to the entire drainage.

Further studies on material from the Seward Glacier and its surrounding bedrock are needed to evaluate the extent of the thermal perturbation related to this area of intense exhumation. A key question is whether higher temperature isotherms are affected and if there is a longer record of exhumation. We studied the zircon U/Pb ages of the Malaspina sediments and also dated several rims using LA-ICP-MS, however we did not find any young ages (none <50 Ma; Enkelmann and others, 2009). Due to the youthfulness of the Yakutat–North American collision in contrast to the India–Asia collision, the tectonic "aneurysm" in the St. Elias syntaxis is presumably younger and might represent a nascent stage (Enkelmann and others, 2009). One of the challenging questions is when the crucial feedbacks developed and if this development was triggered by climatic changes.

Insight on this comes from detrital zircons from the deformed syn-collisional glacial marine and glacial fluvial Yakataga Formation deposits in the fold and thrust belt that yielded an FT age population that peaks at 6 to 5 Ma (Enkelmann and others, 2008, 2009). Taking into account a deposition age of 5 to 4 Ma, these young age populations are comparable to those in the Malaspina sediments today and indicate that a rapidly exhuming source already existed in the Latest Miocene/Pliocene. U/Pb dating on these young FT age zircons suggests the Chugach terrane as the source rock (Enkelmann and others, 2008), which is again similar to the modern Malaspina sediments.

Three-dimensional, fully coupled thermo-mechanical numerical models, conditioned by geological observations, were completed to study the mechanical and thermal evolution of the St. Elias Orogen (fig. A2; Hooks, ms, 2009; Koons and others, 2010). We utilize a commercial finite difference modeling code that simultaneously solves for simple stress-strain relationships, applied kinematic boundary conditions, and heat flow to simulate the mechanical and thermal behavior of Earth materials (Fast Lagrangian Analysis of Continua in 3D ($FLAC^{3D}$); Cundall and Board, 1988; Hooks, ms, 2009; Koons and others, 2010). These continuum mechanics models include standard associated plastic mechanical constitutive models (Mohr-Coulomb and von Mises) and an advective-conductive thermal model. The margins of the models have fixed velocity conditions, and the bottom (400°C at −20 km) and top (0°C) have fixed temperatures. All deformation, including the formation of faults and shear zones, is driven by an applied basal drag on the model Yakutat terrane based upon its observed velocities (Fletcher and Freymueller, 1999). More details on the models are given in the Appendix. The models develop a pattern of strain partitioning characteristic of oblique collisions with a strain maximum associated with the transition of the lateral transform motion to the east (model equivalent of the Fairweather Fault) to contraction within the direction of convergence (the St. Elias fold and thrust belt). The model also reveals that the thermal anomaly at the Yakutat plate corner develops due to the structural geometry and strain concentration that causes rapid vertical motion, and that its position does not change as Yakutat convergence proceeds (Hooks, ms, 2009). This modeling also shows that when erosion is included into the model it increases the rates of vertical motion but does not change the overall geometry. Based on these modeling results and the observed thermochronological data we propose that deep-seated and rapid exhumation at the St. Elias syntaxis (Seward Glacier) has been going on since ca. 5 Ma and thus was not initiated by climate change during the Quaternary. The St. Elias Range is dominated by glaciers today and glaciation has been much more extensive for most of the Quaternary. Glaciers already reached the ocean and provided debris-laden icebergs since 5 Ma (Lagoe and others, 1993). Thus the rapid exhumation might have been initiated by the first glaciation in the region about 5 Ma. It is however likely that the patterns of glacial erosion have changed throughout the glacial-interglacial cycles and as the Yakutat collision evolved, causing changes in drainage areas and the zones where glaciers cut through the southern ranges to reach the Ocean.

There is a significant difference in the exhumation depth between the Himalayan metamorphic massifs and the St. Elias focused erosion. Anatexis and high-grade metamorphic rocks are exposed within the Namche Barwa and Nanga Parbat massifs whereas exhumation in the St. Elias syntaxis area has been less deep, probably affecting only upper and mid-crustal levels. Given the relatively thin crustal section, our inference that rapid exhumation has been underway for some time requires that continued underthrusting is supplying new material to the local crust, and in fact local tectonics suggests that this is the case (for example Fletcher and Freymueller, 1999, 2003; Bruhn and others, 2004; Pavlis and others, 2004; Eberhart-Phillips and others, 2006).

Exhumation in the Fold and Thrust Belt

The thermochronological record of deformed Yakutat cover sediments in the fold and thrust belt deserves a special discussion because they are a major tectonic feature of this collision, and the development of this deformation has important implications for the convergence history. We argue that a synoptic evaluation of these bedrock samples is needed, similar to the approach used with detrital samples, because every apatite grain from these samples originates from a different source area and carries its own cooling history. A critical issue for these potentially shallowly exhumed samples of

sedimentary bedrock is to what degree or not any given grain age might be reset or not. Resetting will depend on the thermal sensitivity of the thermochronometer and the thermal history the sampled sediment experienced since deposition.

Discriminating between reset, non-reset and partially reset ages can be achieved by looking at single grain or single aliquot results of a sample. For helium dating, a large scatter within sample aliquots is generally expected for a sample that is non-reset or partially reset. In a partially reset sample some aliquots will yield ages younger than the depositional age due to partial loss of daughter products, whereby all ages are older than the depositional age in case of a non-reset sample. On the other hand, a fully reset sample is characterized by a good reproducibility of the cooling age that is younger than deposition. In the case of a reset age, the sample can be treated like a general bedrock sample, and the cooling age provides information about timing of last cooling. Any non-reset ages provide information about the cooling history of the source area, but in case of a partially reset sample, the grain ages are not meaningful but the sample does permit an inference about maximum temperature and possibly an inference about maximum burial depth. Zircon U-Th/He dating is usually done on single grains and allow the discrimination between reset, non-reset and partially reset, but all apatite U-Th/He samples from the fold and thrust belt have been analyzed as multi-grain aliquots, which complicates this discrimination (Spotila and others, 2004; Berger and others, 2008a; Berger and Spotila, 2008). A large number of zircon FT data exist from bedrock samples in the active deformed fold and thrust belt of the Yakutat cover strata (Meigs and others, 2008; Perry and others, 2009) and modern fluvial detrital samples from drainages comprised of Yakutat cover strata (Enkelmann and others, 2008, 2009). The ZFT ages reveal that there are no samples in the fold and thrust belt with ages reset in this orogenic cycle. The ages also reveal that lateral transport of sediments into the fold and thrust belt and their exhumation occurred from temperatures insufficient to anneal fission tracks or cause diffusional helium loss in zircon.

A general low geothermal gradient (20-25°C/km) is indicated by thermal studies (vitrinite reflectance and apatite FT) and a detailed knowledge of strata thickness and geometry of the fold and thrust belt (Johnsson and others, 1992; Perry, ms, 2006; Meigs and others, 2008; Perry and others, 2009). These data indicate that most strata in the fold and thrust belt were never hotter than ~100°C, and only locally reached temperatures as high as 180°C (see discussion in Meigs and others, 2008).

Apatite U-Th/He ages from strata of the fold and thrust belt were mostly interpreted as fully reset cooling ages and were used to extract exhumation rates and patterns (Berger and others, 2008a; Berger and Spotila, 2008). This recent work indicated that the Chugach–St. Elias fold and thrust belt was a natural example for tectonic–climate interaction (Berger and others, 2008b). An orogen-parallel narrow band of <1 Ma apatite U-Th/He ages was interpreted as the result of structural reorganization and narrowing of the thrust belt due to Quaternary climate change and glacial intensification (Berger and others, 2008b). We suggest that there is an alternative interpretation for these data. For these ages, we calculated the standard deviation of the component grain ages for each sample, including all measured aliquots. We suspect that those samples with a higher than normal age dispersion (35-150% standard deviation) are not fully reset ages (partially reset) or unreset (fig. 7). Most unreset ages are from the youngest Yakataga Formation, which was buried least in contrast to the stratigraphically older Kultieth and Poul Creek Formations. However, an interesting result of this analysis is that the regional distribution of reset and un-reset ages shows a map-view wedge of reset ages that is bounded to the north by the Chugach–St. Elias fault and thins eastward, suggesting that sediments in the area close to the St. Elias syntaxis and the indenter corner are all exhumed from very

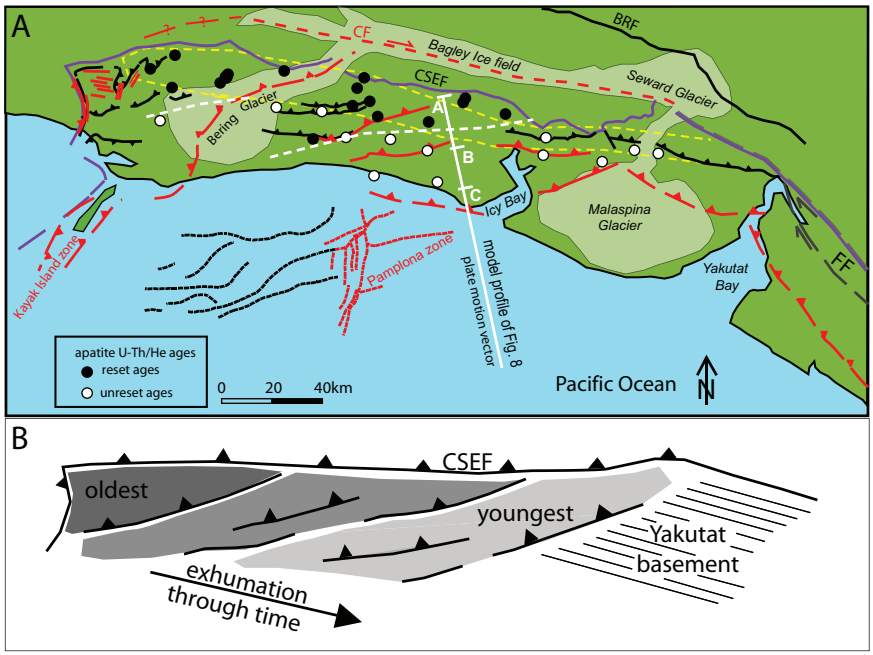

Fig. 7. (A) The Chugach–St. Elias Range with major structures, faults mapped as old (black) and young (red). Dashed lines are assumed faults inferred from seismicity and geological relationships. Apatite U-Th/He samples from Berger and others (2008a), and Berger and Spotila (2008), are plotted, divided into reset and unreset ages. BRF: Border Range Fault, CSEF: Chugach St. Elias Fault, CF: Contact Fault. Yellow dashed line indicates the belt of fastest exhumation as suggested by Berger and Spotila (2008) indicated by <0.75 Ma apatite U-Th/He ages. White dashed line indicates the orientation of packages of rocks that were exhumed from deep and shallow depth as shown in figure 8 (profile is parallel to the Yakutat plate motion vector). (B) Sketch of the re-interpreted exhumation patterns in the fold and thrust belt. Exhumation is oldest in the northwestern part and propagated towards the southeast. The most recent rock exhumation occurs in the southeast as it was also suggested by Meigs and others (2008).

shallow depths (fig. 7). This finding is in agreement with our field observations and work by Plafker (1987) that suggest a general thinning and lack of the older Cenozoic strata (Poul Creek and Kultieth) towards the southeast. Another clue to the significance of this observation is that the Yakutat basement thickens towards the southeast, and is exposed as basement-involved thrust sheets that first appear near Mount St. Elias and become the predominant rock in the thrust belt east of the Seward-Malaspina Glacier system.

The overall age pattern suggests that material exhumed in the northern and central part of the fold and thrust belt is from greater depth, corresponding to temperatures >75°C, whereby material in the south and east of the wedge is from shallower depths. This conclusion is also consistent with mapped surface geology in that thrust sheets throughout this region do not carry syn-orogenic strata, suggesting the leading edges of any of these thrust sheets have been completely exhumed with only the down-dip, deeply exhumed parts of these thrust systems exposed at the surface today. This trend is also supported by three-dimensional mechanical- and thermal modeling of the Chugach–St. Elias orogen (described above and in the Appendix; Hooks, ms, 2009). Temperature–time paths were extracted by using the evolved 3D model velocity field to project particle paths backward in time from a chosen location on the surface of the model. This approach assumes that the time-averaged model

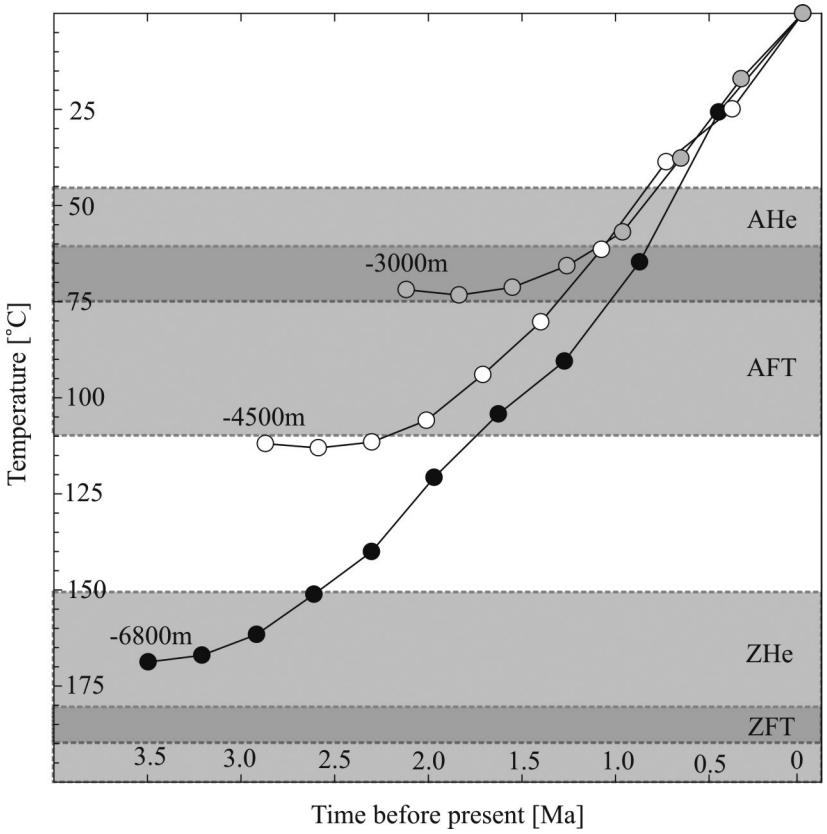

Fig. 8. Modeled temperature–time paths for material exposed in (A) the northern (black circles), (B) central (white circles), and (C) southern (gray circles) part of the fold and thrust belt calculated from the 3D mechanical–thermal model of Hooks (ms, 2009). The orientation of the extracted path is parallel to the GPS plate motion vectors, and shown in figure 7. Details to the model are in the Appendix. Temperature ranges of the thermal sensitivity of the apatite (A) and zircon (Z) fission track (FT) and U-Th/He (He) systems are shown. Location of the profile is shown in figure 7.

velocities have reached steady state conditions and define the flux of material through the orogen. We extracted three temperature–time paths from the model that represents the thermal history of rocks exhumed at the south, central, and northern part of the fold and thrust belt (fig. 8). The model shows that even the northernmost exhumed sample, which started at ~6000 m depth, was never heated to temperatures >175°C, which is in agreement with the non-reset zircon FT ages (Meigs and others, 2008; Perry and others, 2009). The sample exhumed in the south, starting at ~3000 m depth and about 100 km offshore, experienced <75°C during its 2.1 Myr journey. This result means sediments from even shallower depths could never have reached temperatures high enough to reset the apatite U-Th/He system.

We suggest that the exhumation pattern in the fold and thrust belt tracks the northward thickening of the Yakutat cover as it gets continuously accreted to North America, but the data do not reveal a band of margin-parallel rock exhumation presumably due to tectonic reorganization caused by climate change. Our interpretation is in agreement with structural field observations that show young thrust faults mainly in the south and southeast (red lines in fig. 7), which are in a shallow angle to the Chugach–St. Elias fault (suture) and roughly parallel to the reset/non-reset

boundary. Meigs and others (2008) first suggested a southward progression of thrusting based on thermochronology of the Yakutat sediments. In contrast, the suggested band of Quaternary exhumation (Berger and others, 2008b) is parallel to the suture and in an angle to the observed active thrust faults in the field, and to the area of high vertical velocity predicted by the mechanical model (Hooks, ms, 2009).

Exhumation Prior to Yakutat Collision

The modern fluvial detrital samples collected from glacial drainages located north of the Bagley Ice field provide insight into the cooling history of the Chugach terrane [fig. 4B and table DR3 (http://earth.geology.yale.edu/~ajs/SupplementaryData/2010/03EnkelmannTableDR3.pdf); Enkelmann and others, 2008]. All zircon FT ages are interpreted as cooling ages due to exhumation, and are not thermally affected by hot fluids, or young magmatism. This assumption is supported by our field observations and FT and U/Pb double dating of modern fluvial detrital zircons that yield much older crystallization ages than FT cooling ages (Enkelmann and others, 2008). The oldest zircon FT age peaks range from 42 to 35 Ma and record the middle Eocene cooling after ridge subduction and associated granitic intrusions (fig. 5; Enkelmann and others, 2008). Younger detrital grain age populations in the Chugach terrane range from 35 to 8 Ma and are much younger than the few bedrock apatite and zircon ages that exist for this area (fig. 4). The zircon FT data reveal that exhumation of the Chugach terrane started in the late Eocene to early Oligocene, coinciding with the beginning of the northward transport of the Yakutat terrane and may record the onset of flat-slab subduction (fig. 9; Plafker and others, 1994). This onset of Chugach terrane exhumation is also supported by the beginning of sedimentation in the Cook Inlet and Copper River Basin (Flores and others, 2004; Trop and others, 2004). The detrital zircon FT data show two phases of exhumation that followed at ~20 Ma and ~11 Ma and coincided with changes in the Pacific plate motion (Stock and Molnar, 1988). Generally, the youngest cooling ages are under the Bagley Ice field and the area just north of it and ages become older towards the north with no significant exhumation north of the Border Range fault since the Early Cretaceous (Enkelmann and others, 2008). Evidence for these Miocene pulses of exhumation in the Chugach terrane is also preserved by the unreset zircon ages of the syn-orogenic Yakataga Formation located in the fold and thrust belt (fig. 4; Enkelmann and others, 2008; Perry and others, 2009). It has been shown that the zircon FT age populations as well as the petrography of the Yakataga Formation sediments are comparable to Chugach metamorphic complex and that this was a major sediment source in the Pliocene (Perry, ms, 2006; Enkelmann and others, 2008). A recent zircon U-Th/He and U/Pb analysis of granitic and gneissic clasts from the Yakataga Formation also show a clear Chugach terrane source with Miocene cooling ages (Witmer and others, 2009). Together, the thermochronological and sedimentological data imply that the Chugach terrane was uplifted and experienced erosion and rock exhumation prior to the Yakutat collision with Wrangellia as the backstop. Considering only the zircon FT cooling ages shown in figure 9 we can predict that the age of the onset of exhumation and related sediments is ca. 26 Ma in the late Oligocene.

CONCLUSIONS

The thermochronology in southeast Alaska reveals that the climate influence on the pattern of erosion is limited and localized (only along the coast side of the mountain range), and that the location of significant rock exhumation from deeper crustal levels is primarily influenced by tectonic processes that develop a coupling with surface processes. There are large variations in exhumation patterns along orogenic strike that show a clear culmination at the Yakutat tectonic corner, the region of the St.

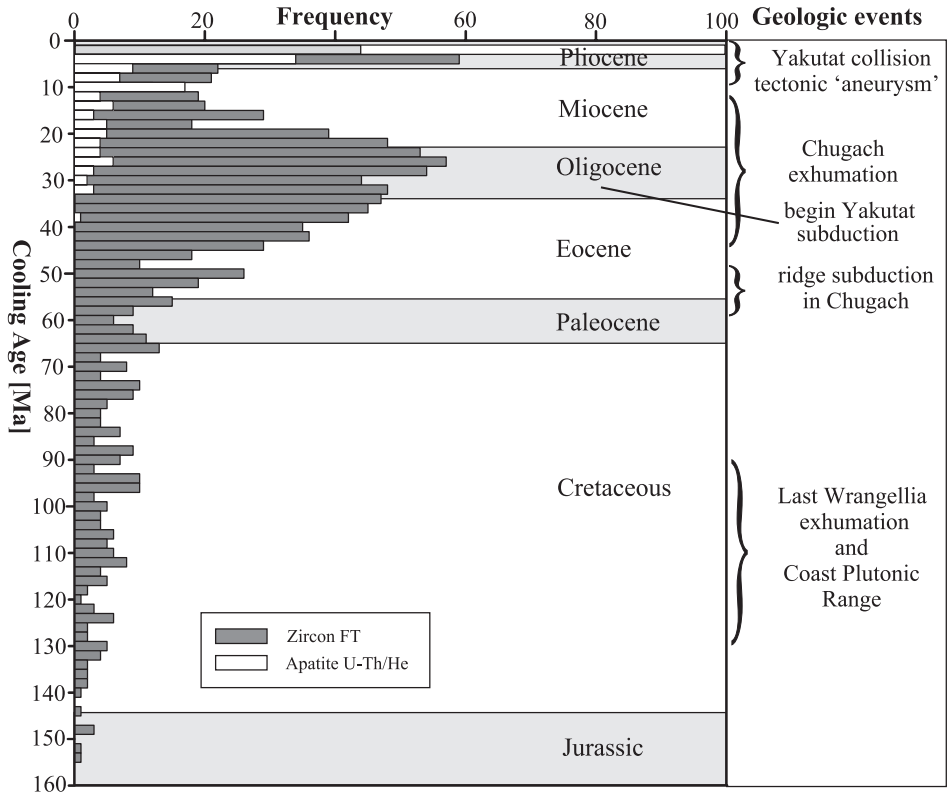

Fig. 9. Summary of the thermochronological record of southeast Alaska. Histogram shows modern fluvial detrital zircon FT analysis (N=1164; data from Enkelmann and others, 2008, 2009, and this study), and single aliquot apatite U-Th/He analysis from bedrock samples including the fold and thrust belt (N=243; data from Spotila and others, 2004; Berger and others, 2008a; Berger and Spotila, 2008).

Elias syntaxis. The structural, topographic, and thermochronological observations at the St. Elias syntaxis are very similar to those of the Himalayan syntaxes and suggest that the development of the localized thermal perturbation in the crust and ensuing feedbacks can be fast and does not require long lasting subduction of thick continental crust. The development of the tectonic "aneurysm" at the St. Elias syntaxis does not seem to be affected or initiated by climatic change in the Quaternary. The same is true for the development of the fold and thrust belt, as suggested by our re-interpretation of apatite U-Th/He ages. The most recently exhumed rocks within the thrust belt are located close to the St. Elias syntaxis and originate from a very shallow depth.

We propose that the southeastern margin of Alaska has been actively uplifted, eroded, and exhumed since the beginning of the Yakutat lithosphere subduction in the Oligocene. Several phases of Oligocene and Miocene exhumation are recorded by cooling ages of the rocks in the Chugach terrane and correlate with the onset of sedimentation in the Cook Inlet and Copper River basin (fig. 9). The overall exhumation patterns in southeast Alaska are summarized in figure 10. Besides the region of the St. Elias syntaxis, and the fold and thrust belt exhumation is concentrated along the Fairweather fault. The Chugach terrane rocks of the Chugach–St. Elias range are still actively eroding but to a less amount than the southern flanks of the range, where erosion rates are high but exhumation is shallow due to the lateral transport of

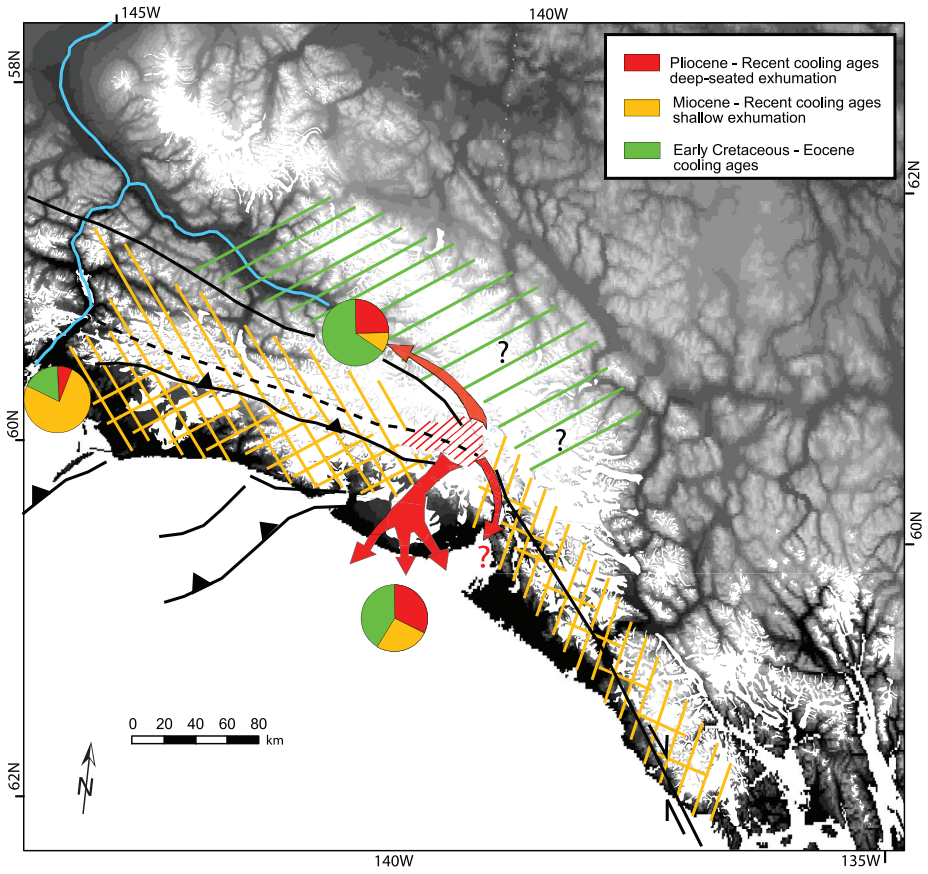

Fig. 10. Summary of exhumation pattern in southeast Alaska. Pie charts show composition of the sand sample from the upper Chitina River and the Copper River delta, based on zircon FT age populations.

material in the fold and thrust belt. This shallow exhumation of material in an accretionary wedge has been shown previously by 2D numerical models for the Olympic Mountains (Batt and others, 2001), and is shown here by 3D models for the Yakutat–North American collision. Since the Early Cretaceous, the Wrangellia terrane formed the backstop for terrane accretion and the area north of the Chugach–St. Elias range and the St. Elias syntaxis (Wrangell Mountains) is just recently uplifted and eroded as a consequence of the continuing Yakutat collision. More research is necessary in the Wrangell Mountains to quantify the exhumation and the beginning, as well as the influence of the volcanism that affects this area since the Miocene.

ACKNOWLEDGMENTS

We thank collaborators of the STEEP project for their help during field work and fruitful discussions. We also thank J. Spotila for providing sample separates. We are thankful to the U.S. D.O.E. reactor use sharing program (Oregon State University) for fission track irradiation and the McMaster irradiation facility for $^{40}Ar/^{39}Ar$ study. The manuscript was improved by constructive reviews by Peter van der Beek and Stuart N. Thomson. This study was supported by the NSF grants, EAR-0409132 and 0735402.

Appendix

new thermochronological data

Methods

U-Th/He analysis.—Rock samples were crushed, sieved and washed to extract a grain size that ranges from 60 to 250 μm. Apatite and zircons were crystals without inclusions, cracks, or other defects that were selected under a binocular microscope at nominal magnification of 100x. Grain diameters range from 80 to 150 μm for apatite, and 75 to 125 μm for zircons. Aliquots of multiple apatite grains and single zircon grains were analyzed for ^{4}He in the noble gas laboratory at Lehigh University. Apatite and zircon grains were heated in a resistance furnace at 1100°C for 15 minutes and 1350°C for 60 minutes, respectively, and analyzed for ^{4}He by isotope dilution utilizing a ^{3}He spike and quadrupole mass spectrometry. After helium analysis, the samples were sent to the University of Arizona at Tucson for uranium, thorium, and samarium measurements using isotope-dilution ICP-MS. The analytical error of isotope measurements using mass spectrometry is small (1-2%). Because intra-sample error (analytical reproducibility) is much larger than the analytical error, the error reported for each sample reflects that of the error in sample replication. The errors in table 1 are calculated as the simple standard deviation of the sample age population. Analytical details of individual samples are presented in supplemental data tables DR1 and DR2 (http://earth.geology.yale.edu/~ajs/SupplementaryData/2010/01EnkelmannTableDR1.pdf; http://earth.geology.yale.edu/~ajs/SupplementaryData/2010/02EnkelmannTableDR2.pdf).

^{40}Ar/^{39}Ar analysis.—Potassium feldspar was separated from two coarse-grained granitic rocks of the Wrangellia composite terrane. After crushing we handpicked 8 to 22 mg of pure K-feldspar grains under the binocular microscope and packed them in pure copper foil for neutron irradiation at the McMaster reactor. Argon analysis was carried out in the noble-gas laboratory at Lehigh University. The argon gas was extracted by stepwise heating of the sample packages using a double-vacuum resistance furnace. Each sample was heated in 58 steps ranging from 400 to 1500°C, and varying durations of 15 minutes to 2 hours. Isotope ratios were measured with a VG 3600 noble-gas mass spectrometer using an electron-multiplier detector. Standard step-heating analytical data are given in supplemental data table DR4 (http://earth.geology.yale.edu/~ajs/SupplementaryData/2010/04EnkelmannTableDR4.pdf).

Figure A1 shows the age spectra for samples EUT-35 and EUT-2 as well as the results from inverse modeling of the age spectra for thermal history, using kinetics and domain structures derived from each sample's ^{39}Ar release during step heating analysis [table DR5 (http://earth.geology.yale.edu/~ajs/SupplementaryData/2010/05EnkelmannTableDR5.pdf)]. Modeling of the sample's gas release indicates the presence of several diffusion domains that have slow cooling closure temperatures ranging from 165 to 290°C (EUT-2) or 210 to 335°C (EUT-35). Despite small discordance overall the age spectra are flat and indicate that relatively fast cooling through this temperature range occurred at about 130 Ma. The age spectra for both samples are remarkably free from any excess argon expressed early in gas release as is typical for most samples, and the earliest gas released gives ages as young as about 50 to 60 Ma (this age is hard to resolve any better given the uncertainties in the small gas fractions and the asymptotic approach of the age spectrum to the age axis).

This qualitative conclusion is supported by inverse modeling using the Arvert 4 code (Zeitler, 2004; Harrison and others, 2005). The inversions, which use a controlled-random-search algorithm and which permit reheating as well as cooling, are dominated by monotonic cooling with closure for most domains in the interval about 130 to 140 Ma (EUT-2) or about 125 Ma (EUT-35), at rates of ~20°C/.y. (EUT-2) or possibly much more (EUT-35) (the slightly discordant nature of the age spectra preclude a more definitive statement about rate). The combination of this early closure to temperatures below about 200°C, plus the later closure of the least retentive domains, suggest that the samples remained warm with little movement towards the surface for many tens of million years after initial rapid cooling.

Detrital zircon FT analysis.—Detrital zircons were separated from sand samples of the Chitina and Copper River using standard magnetic and heavy liquid techniques. Zircon fission track dating has been carried in the same procedure as for the other detrital samples of southeast Alaska published in Enkelmann and others, (2008, 2009). For each sample we dated more than 100 single grains. Grain-age distributions were deconvolved into component age populations using binomial peak-fitting (table 2; Galbraith and Green, 1990; Brandon and others, 1992, 1996). Single grain ages are shown in age groups in figure 4 and age populations in figure 10.

published thermochronology

Previously published thermochronology is given in supplemental data table DR3, http://earth.geology.yale.edu/~ajs/SupplementaryData/2010/03EnkelmannTableDR3.pdf. The average age and standard deviation in table DR3 are those reported in the original publication.

3d thermo-mechanical numerical models

Three-dimensional, coupled thermal-mechanical numerical models were constructed to study orogen scale kinematics and dynamics during the evolution of the St. Elias Orogen, southern Alaska (Hooks, 2009;

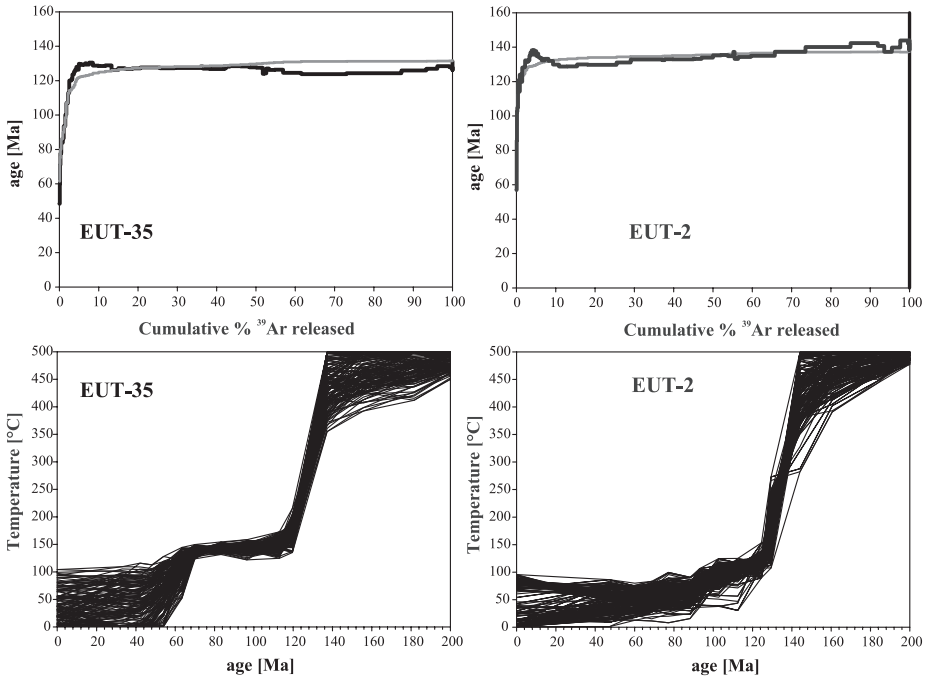

Fig. A1. Results of potassium-feldspar $^{40}Ar/^{39}Ar$ analysis, samples EUT-35 and EUT-2. Top panel: measured age spectra (dark) and mean of inversion models (gray). Bottom: Plot of thermal histories, showing bundles of 150 thermal histories (all histories converged to an acceptably grouped but not statistical fit (mean percent deviation) of 3.8% or better given the mildly discordant nature of the age spectra. The inversion for EUT-35 permitted only monotonic cooling; for EUT-2 mild reheating of 5°C/m.y. was permitted.

Koons and others, 2010). These models allow for the testing of the influence of boundary, surface, and geometric characteristics on the evolution of plate corner within a continuum mechanics framework. The model geometry encompasses an area of dimensions 890 km (north-south=Y) by 640 km (east-west=X) with a thickness of 20 km (=Z) (fig. A2). An isotropic conductive-advective thermal model (thermal conductivity (k) = 2.6 Wm-1C-1; radiogenic volumetric heat source (Av) = 0.37 μWm-3) and Mohr-Coulomb (~upper 15 km; φ = 30; cohesion = 44 MPa) and thermally-defined plastic yield condition (~lower 5 km; yield strength = 100 MPa) mechanical models are used to define the thermal and mechanical constitutive models. The models include no initial weaknesses; faults and shear zones develop as the model evolves as a function of partitioning and focusing of strain.

The initial velocity conditions are imposed on the base of the model over an area corresponding to the spatial extent of the Yakutat terrane (south of the Chugach–St. Elias Fault and west of the Fairweather Fault) consistent with its observed motions (~50 mm/yr; Fletcher and Freymueller, 2003). All margins of the model, except the surface, have fixed velocity conditions. The top and bottom (−20 km) of the model are conditioned with fixed temperatures of 0 and 400°C, respectively (fig. A2).

The modeling path first develops a reference Tectonic Model in the absence of topography or erosion; then the natural topography (Topographic Model) and an erosion scheme (Erosion Model) are successively applied as initial boundary conditions. The present topography, including bathymetry, was derived from a global 1-minute DEM sampled at the model discretization (~10 km spacing; Smith and Sandwell, 1997). The presence of anomalous topography has been shown to alter the stress state of the crust and can lead to feedback between uplift and localization of strain (Koons and others, 2002). To emphasize the influence of erosion, vigorous erosional conditions are applied based upon the spatial extent of current glaciations and are based on the assumption that glacial erosion maintains a near constant elevation during exhumation (Hallet and others, 1996; Meigs and Sauber, 2000). The erosion model employed for this study maintains the model nodes at a constant elevation (fixed between 500 and 1000 m) within the defined zone of erosion

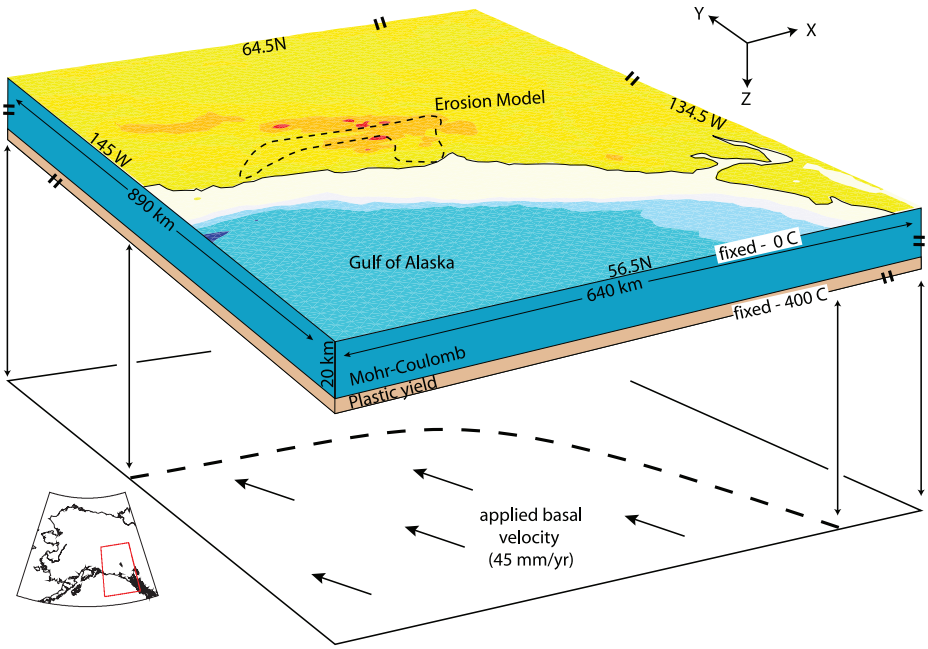

Fig. A2. Model diagram showing 3D geometry and boundary conditions for the numerical model (modified from Hooks, ms, 2009). Not all model boundaries have fixed velocity conditions, except the model surface, which is free to deform. The model surface is conditioned with natural topography (color fill; 1000 m contours) and an erosion model (see the dashed outline) that maintains a constant topography by removing material from the surface. A basal drag is applied to the model over the area of the Yakutat Terrane (see drop down plane) by giving the area the observed velocity of the Yakutat Terrane (~45 mm/yr). The model surface and base (~20 km depth) are given fixed temperatures of 0°C and 400°C, respectively.

during the model run. Material passing through the model surface at these zones is essentially removed from the model system.

Hooks (ms, 2009) shows that the resultant deformation patterns produced by the model are relatively insensitive to the initial surface boundary conditions (that is erosion and topography). This suggests that the strain patterns observed within the orogen are primarily controlled by the kinematics and tectonic geometry. As the models reproduce the uplift and strain patterns observed within southern Alaska (Hooks, ms, 2009; Koons and others, 2010), it is assumed that the model kinematic conditions are aptly characterized.

Backward projections of particle paths are extracted from the model. This technique assumes that the velocity conditions have reached near steady-state conditions and define the flux of material through the orogen (Hooks, ms, 2009). Three particle paths were extracted from three locations of exhumation (A, B, and C on fig. 7). Temperatures and velocity conditions we re-extrapolated from the model grid to yield the three-dimensional paths extrapolated to the depth reach near constant values. Times were calculated using the velocities along the paths.

References

Barker, F., Farmer, G. L., Ayuso, R. A., Plafker, G., and Lull, J. S., 1992, The 50 Ma granodiorite of the eastern Gulf of Alaska: Melting in an accretionary prism in the forarc: Journal of Geophysical Research, v. 97, n. B5, p. 6757–6778, doi:10.1029/92JB00257.

Batt, G. E., and Brandon, M. T., 2002, Lateral thinking: 2-D interpretation of thermochronology in convergent orogenic settings: Tectonophysics, v. 349, p. 185–201, doi:10.1016/S0040-1951(02)00053-7.

Batt, G. E., Brandon, M. T., Farley, K. A., and Roden-Tice, M., 2001, Tectonic synthesis of the Olympic Mountains segment of the Cascadia wedge, using two-dimensional thermal and kinematic modeling of thermochronological ages: Journal of Geophysical Research, v. 106, B11, p. 26,731–26,746, doi:10.1029/2001JB000288.

Beaumont, C., Fullsack, P., and Hamilton, J., 1992, Erosional control of active compressional orogens, *in* McClay, K. R., editor, Thrust Tectonics: New York, Chapman and Hall, p. 1–18.
Berger, A. L., and Spotila, J. A., 2008, Denudation and deformation in a glaciated orogenic wedge: The St. Elias orogen, Alaska: Geology, v. 36, p. 523–526, doi:10.1130/G24883A.1.
Berger, A. L., Spotila, J. A., Chapman, J. B., Pavlis, T. L., Enkelmann, E., Ruppert, N. A., and Buscher, J. T., 2008a, Architecture, kinematics, and exhumation of a convergent orogenic wedge: A thermochronological Investigation of tectonic-climatic interactions within the central St. Elias Orogen, Alaska: Earth and Planetary Science Letters, v. 270, p. 13–24, doi:10.1016/j.epsl.2008.02.034.
Berger, A. L., Gulick, S. P. S., Spotila, J. A., Upton, P., Jaeger, J. M., Chapman, J. B., Worthington, L. A., Pavlis, T. L., Ridgway, K. D., Willems, B. A., and McAleer, R. J., 2008b, Quaternary tectonic response to intensified glacial erosion in an orogenic wedge: Nature Geoscience, v. 1, p. 793–796, doi:10.1038/ngeo334.
Booth, A. L., Chamberlain, P. C., Kidd, W. S. F., and Zeitler, P. K., 2009, Constraints on the metamorphic evolution of the eastern Himalayan syntaxis from geochronologic and petrologic studies of Namche Barwa: Geological Society of America Bulletin, v. 121, p. 385–407, doi: 10.1130/B26041.1.
Brandon, M. T., 1996, Probability density plot for fission track grain-age samples: Radiation Measurements, v. 26, p. 663–676, doi:10.1016/S1350-4487(97)82880-6.
Brandon, M. T., Roden-Tice, M. K., and Garver, J. I., 1998, Late Cenozoic exhumation of the Cascadia accretionary wedge in the Olympic Mountains, northwest Washington State: Geological Society of America Bulletin, v. 110, p. 985–1009, doi:10.1130/0016-7606(1998)110<0985:LCEOTC>2.3.CO;2.
Brocklehurst, S. H., and Whipple K. X., 2002, Glacial erosion and relief production in the eastern Sierra Nevada, California: Geomorphology, v. 42, p. 1–24, doi:10.1016/S0169-555X(01)00069-1.
——— 2007, Response of glacial landscapes to spatial variations in rock uplift rate: Journal of Geophysical Research, v. 112, p. F02035, doi:10.1029/2006JF000667.
Bruhn, R. L., Pavlis, T. L., Plafker, G., and Serpa, L., 2004, Deformation during terrane accretion in the Saint Elias orogen, Alaska: Geological Society of America Bulletin, v. 116, p. 771–787, doi:10.1130/B25182.1.
Carlson, W. D., Donelick, R. A., and Ketcham, R. A., 1999, Variability of apatite fission track annealing kinetics: I. Experimental Results: American Mineralogist, v. 84, p. 1213–1223.
Christeson, G. L., van Avendonk, H., Gulick, S. P., Worthington, L., and Pavlis, T., 2008, Crustal structure of the Yakutat microplate: constraints from STEEP wide-angle seismic data: Eos Transactions, AGU 89(53), Fall Meeting Supplement, Abstract T53B-1942.
Conway, H., Smith, B., Vaswani, P., Matsuoka, K., Rignot, E., and Claus P., 2009, A low-frequency ice-penetrating radar system adapted for use from an airplane: test results from Bering and Malaspina Glaciers, Alaska: Annals of Glaciology, v. 50, p. 93–97, doi: 10.3189/172756409789097487.
Cowan, D. S., 2003, Revisiting the Baranof–Leech River hypothesis for early Tertiary coastwise transport of the Chugach–Prince William terrane: Earth and Planetary Science Letters, v. 213, p. 463–475, doi: 10.1016/S0012-821X(03)00300-5.
Cundall, P. A., and Board, M., 1988, A microcomputer program for modeling large-strain plasticity problems, *in* Swododa, C., editor, Numerical Methods in Geomechanics, Proceedings of the 6th International Conference on Numerical Methods in Geomechanics, Innsbruck, Austria, April 11–15: Rotterdam, Balkema, p. 2101–2108.
Dodson, M. H., 1973, Closure temperature in cooling geochronological and petrological systems: Contributions to Mineralogy and Petrology, v. 40, p. 259–274, doi:10.1007/BF00373790.
Eberhart-Phillips, D., Christensen, D. H., Brocher, T. M., Hansen, R., Ruppert, N. A., Haeussler, P. J., and Abers, G. A., 2006, Imaging the transition from Aleutian subduction to Yakutat collision in central Alaska, with local earthquakes and active source data: Journal of Geophysical Research, v. 111, p. B11303, doi:10.1029/2005JB004240.
Elliott, J., Freymueller, J. T., and Larsen, C. F., 2008, Collisional Tectonics in the St. Elias orogen, Alaska, observed by GPS: Eos Transactions, AGU 89 Fall Meeting Supplement, Abstract T44A-04.
Enkelmann, E., Garver, J. I., and Pavlis, T. L., 2008, Rapid exhumation of ice-covered rocks of the Chugach-St. Elias orogen, Southeast Alaska: Geology, v. 36, p. 915–918, doi:10.1130/G2252A.1.
Enkelmann, E., Zeitler, P. K., Pavlis, T. L, Garver, J. I., and Ridgway, K. D., 2009, Intense Localized Rock Uplift and Erosion in the St. Elias Orogen of Alaska: Nature Geoscience, v. 2, p. 360–363, doi:10.1038/ngeo502.
Ferris, A., Abers, G. A., Christensen, D. H., and Veenstra, E., 2003, High resolution image of the subducted Pacific (?) plate beneath central Alaska, 50–150 km depth: Earth and Planetary Science Letters, v. 214, p. 575–588, doi:10.1016/S0012-821X(03)00403-5.
Finnegan, N. J., Hallet, B., Montgomery, D. R., Zeitler, P. K., Stone, J. O., Anders, A. M., and Yuping, L., 2008, Coupling of rock uplift and river incision in the Namche Barwa–Gyala Peri massif, Tibet: Geological Society of America, v. 120, p. 142–155, doi:10.1130/B26224.1.
Fletcher, H. J., and Freymueller J. T., 1999, New GPS constraints on the motion of the Yakutat block: Geophysical Research Letters, v. 19, p. 3029–3032, doi:10.1029/1999GL005346.
——— 2003, New constraints on the motion of the Fairweather fault, Alaska, from GPS observations: Geophysical Research Letters, v. 30, p. 1139, doi:10.1029/2002GL016476.
Flores, R. M., Stricker, G. D., and Kinney, S. A., 2004, Alaska Coal Geology, Resources, and Coalbed Methane Potential: U.S. Geological Survey DDS-77, 125 p., 3 sheets.
Freymueller, J. T., Woodard, H., Cohen, S. C., Cross, R. S., Elliott, J., Larsen, C. F., Hreinsdottir, S., and Zweck, C., 2008, Active deformation processes in Alaska, based on 15 years of GPS measurements, *in* Freymueller, J. T., Haeussler, P. J., Wesson, R. L., and Ekström, G., editors, Active Tectonics and Seismic Potential of Alaska: Geophysical Monograph Series, v. 179, p. 1–42.
Fuis, G. S., Moore, T. E., Plafker, G., Brocher, T. M., Fisher, M. A., Mooney, W. D., Nokleberg, W. J., Page, R. A., Beaudoin, B. C., Christensen, N. I., Levander, A. R., Lutter, W. J., Saltus, R. W., and Ruppert, N. A.,

2008, Trans-Alaska crustal transect and continental evolution involving subduction underplating and synchronous foreland thrusting: Geology, v. 36, p. 267–270, doi:10.1130/G24257A.1.
Galbraith, R. F., and Green, P. F., 1990, Estimating the component ages in a finite mixture: Nuclear Tracks and Radiation Measurements, v. 17, p. 197–206, doi:10.1016/1359-0189(90)90035-V.
Green, P. F., Duddy, I. R., Gleadow, A. J. W., Tingate, P. T., and Laslett, G. M., 1986, Thermal annealing of fission tracks in apatite: 1. A qualitative description: Chemical Geology: Isotopic Geoscience section, v. 59, p. 237–253, doi:10.1016/0168-9622(86)90074-6.
Gulick, S. P. S., Pavlis, T. L., Christeson, G., Jaeger, J. M., Ridgway, K. D., Worthington, L., Reece, R. S., and Horton, B. K., 2009, Marine records of flat slab subduction influenced by temperate glaciations in the St. Elias orogen, Gulf of Alaska: GSA Annual Meeting, Portland, Abstact No. 108-17.
Hallet, B., Hunter, L., and Bogen, J., 1996, Rates of erosion and sediment evacuation by glaciers: A review of field data and their implications: Global and Planetary Change, v. 12, p. 213–235, doi:10.1016/0921-8181(95)00021-6.
Harrison, T. M., Grove, M., Lovera, O. M., and Zeitler, P. K., 2005, Continuous thermal histories from inversion of closure profiles, *in* Reiners, P. W., and Ehlers. T. A., editors, Low-Temperature Thermochronology: Techniques, Interpretations, and Applications: Reviews in Mineralogy and Geochemistry, v. 58, p. 389–409, doi: 10.2138/rmg.2005.58.15.
Headley, R., Hallet, B., and Rignot, E., 2007, Measurements of Fast ice Flow of the Malaspina Glacier to Explore Connections Between Glacial Erosion and Crustal Deformation in the St. Elias Mountains, Alaska: Eos Transactions, AGU, 88(52), Fall Meeting Supplement, Abstract C41A-0050.
Hooks, B. P., ms, 2009, Geodynamics of terrane accretion within southern Alaska: Orono, Maine, University of Maine, Ph. D. thesis, 188 p.
Hooks, B. P., Enkelmann, E., Koons, P. O., and Upton, P., 2009, 3D thermomechanical modeling of the St. Elias Tectonic aneurysm: Geological Society of America Abstracts with Programs, v. 41, n. 7, p. 305.
Hudson, T., 1983, Calk-alkaline plutonism along the Pacific rim of southern Alaska, *in* Roddick, J. A., editor, Circum-Pacific plutonic terranes: Boulder, Colorado, GSA Memoir, v. 159, p. 159–169.
Hudson, T., Plafker, G., and Rubin, M., 1976, Uplift rates of marine terrace sequences in the Gulf of Alaska, *in* Cobb, E. H., editor, The United States Geological Survey in Alaska: Accomplishments during 1975: Denver, Colorado, United States Geological Survey, p. 11–13.
Johnsson, M. J., Pawlewicz, M. J., Harris, A. G., and Valin, Z. C., 1992, Vitrinite reflectance and conodont color alteration index data from Alaska: data to accompany the thermal maturity map of Alaska: USGS Open-File Report 92–409.
Kalbas, J. L., Freed, A. M., and Ridgway, K. D., 2008, Contemporary fault mechanics in Southern Alaska, *in* Freymueller, J. T., Haeussler, P. T., Wesson, R., and Ekström, G., editors, Active Tectonics and Seismic Potential of Alaska: Geophysical Monograph Series, v. 179, p. 321–336.
Koons, P. O., 1987, Some thermal and mechanical consequences of rapid uplift: An example from the Southern Alps, New Zealand: Earth and Planetary Science Letters, v. 86, p. 307–319, doi:10.1016/0012-821X(87)90228-7.
——— 1990, Two-sided orogeny; Collision and erosion from the sandbox to the Southern Alps, New Zealand: Geology, v. 18, p. 679–682, doi:10.1130/0091-7613(1990)018<0679:TSOCAE>2.3.CO;2.
Koons, P. O., Zeitler, P. K., Chamberlain, C. P., Craw, D., and Meltzer, A. S., 2002, Mechanical links between erosion and metamorphism in Nanga Parbat, Pakistan Himalaya: American Journal Science, v. 302, p. 749–773, doi:10.2475/ajs.302.9.749.
Koons, P. O., Hooks, B. P., Pavlis, T., and Upton, P., and Barker, A. D., 2010, Three-dimensional mechanics of Yakutat convergence in the southern Alaskan plate corner: Tectonics, doi:10.1029/2009TC002463.
Korup, O., and Montgomery, D. R., 2008, Tibetan plateau river incision inhibited by glacial stabilization of the Tsangpo gorge: Nature, v. 455, p. 786–789, doi:10.1038/nature07322.
Lagoe, M. B., and Zellers, S. D., 1996, Depositional and microfaunal response to Pliocene climate change and tectonics in the eastern Gulf of Alaska: Marine Micropaleontology, v. 27(1-4), p. 121–140, doi: 10.1016/0377-8398(95)00055-0.
Lagoe, M. B., Eyles, C. H., Eyles, N., and Hale, C., 1993, Timing of late Cenozoic tidewater glaciation in the far North Pacific: Geological Society of America Bulletin, v. 105, p. 1542–1560, doi:10.1130/0016-7606(1993)105<1542:TOLCTG>2.3.CO;2.
Lahr, J. C., and Plafker, G., 1980, Holocene Pacific-North American plate interaction in southern Alaska: Implications for the Yakataga seismic gap: Geology, v. 8, p. 483–486, doi:10.1130/007613(1980)8<483:HPAPII>2.0.CO;2.
Larsen, C. F., Motyka, R. J., Freymueller, J. T., Echelmeyer, K. A., and Ivins, E. R., 2004, Rapid uplift of southern Alaska caused by recent ice loss: Geophysical Journal International, v. 158, p. 1118–1133, doi:10.1111/j.1365-246X.2004.02356.x.
Lock, J., and Willett, S., 2008, Low-temperature thermochronometric ages in fold-and-thrust belts: Tectonophysics, v. 456, p. 147–162, doi:10.1016/j.tecto.2008.03.007.
Lowe, L. A., Gulick, S. P., Christeson, G. L., van Avendonk, H., Reece, R., Elmore, R., and Pavlis, T., 2008, Crustal structure and deformation of the Yakutat microplate: New insights from STEEP marine seismic reflection data: Eos Transactions, AGU 89 (53), Fall Meeting Supplement, Abstract 236 T53B-1941.
MacKevett, E. M., Jr., 1978, Geologic map of McCarthy quadrangle, Alaska: U.S. Geological Survey Miscellaneous Geologic Investigations Map I-1032, 1 sheet, scale 1:250,000.
Mancktelow, N. S., and Graseman, B., 1997, Time-dependent effects of heat advection and topography on cooling histories during erosion: Tectonophysics, v. 270, p. 167–195, doi:10.1016/S0040-1951(96)00279-X.
McAleer, R. J., Spotila, J. A., Enkelmann, E., and Berger, A. L., 2009, Exhumation along the Fairweather Fault, Southeast Alaska, based on Low-Temperature Thermochronometry: Tectonics, v. 28, p. TC1007, doi:10.1029/2007TC002240.

Meigs, A., and Sauber, J., 2000, Southern Alaska as an example of the long-term consequences of mountain building under the influence of glaciers, *in* Stewart, I. S., Sauber, J., and Rose, J., editors, Glacio-seismotectonics; ice sheets, crustal deformation and seismicity: Quaternary Science Reviews, v. 19, n. 14, p. 1543–1562.

Meigs, A., Johnston, S., Garver, J., and Spotila, J., 2008, Crustal-scale structural architecture, shortening, and exhumation of an active, eroding orogenic wedge (Chugach/St. Elias Range, southern Alaska): Tectonics, v. 27, p. TC4003, doi:10.1029/2007TC002168.

Nokleberg, W. J., Plafker, G., and Wilson, F. H., 1994, Geology of south-central Alaska, *in* Plafker, G., and Berg, H. C., editors, The Geology of Alaska: Boulder, Colorado, Geological Society of America, Geology of North America, v. G-1, p. 311–366.

O'Sullivan, P. B., and Currie, L. D., 1996, Thermotectonic history of Mt. Logan, Yukon Territory, Canada: implications of multiple episodes of middle to late Cenozoic denudation: Earth and Planetary Science Letters, v. 144, p. 251–261, doi:10.1016/0012-821X(96)00161-6.

O'Sullivan, P. B., Plafker, G., and Murphy, J. M., 1997, Apatite Fission-Track Thermotectonic History of Crystalline Rocks in the Northern Saint Elias Mountains, Alaska, *in* Dumoulin, J. A., and Gray, J. E., editors, Geological studies in Alaska by the United States Geological Survey, 1995: United States Geological Survey Professional Paper, v. 1574, p. 283–294.

Page, R. A., 1969, Late Cenozoic movement on the Fairweather Fault in Southeast Alaska: Geological Society of America Bulletin, v. 80, p. 1873–1878, doi:10.1130/0016-7606(1969)80[1873:LCMOTF]2.0.CO;2.

Pavlis, T. L., and Roeske, S. M., 2007, The Border Ranges fault system, southern Alaska, *in* Ridgway, K. D., Trop, J. M., Glen, J. M. G., and O'Neill, J. M., editors, Tectonic Growth of a Collisional Continental Margin: Crustal Evolution of Southern Alaska: Geological Society of America Special Paper, v. 431, p. 95–127, doi:10.1130/2007.2431(05).

Pavlis, T. L., Marty, K., and Sisson, V. B., 2003, Constrictional flow within the Eocene forearc of Southern Alaska; An effect of dextral shear during ridge subduction, *in* Sisson, V. B., Roeske, S. M., and Pavlis, T. L., editors, Geology of a transpressional orogen developed during ridge-trench interaction along the Pacific margin: Geological Society of America Special Paper, v. 371, p. 171–190, doi:10.1130/0-8137-2371-X.171.

Pavlis, T. L., Picornell, C., Serpa, L., Bruhn, R. L., and Plafker, G., 2004, Tectonic processes during oblique collision: Insights from the St. Elias orogen, northern North American Cordillera: Tectonics, v. 23, p. TC3001, doi:10.1029/2003TC001557.

Perry, S. E., ms, 2006, Thermochronology and provenance of the Yakutat terrane, southern Alaska based on fission-track and U/Pb analysis of detrital zircon: State University of New York at Albany, M.S. thesis, 167 p.

Perry, S. E., Garver, J. I., and Ridgway, K. D., 2009, Transport of the Yakutat Terrane, Southern Alaska: Evidence from Sediment Petrology and Detrital Zircon Fission-Track and U/Pb Double Dating: The Journal of Geology, v. 117, p. 156–173. doi:10.1086/596302.

Péwé, T. L., 1975, Quaternary geology of Alaska: U.S. Geological Survey Professional Paper, v. 835, 139 p.

Plafker, G., 1987, Regional geology and petroleum potential of the northern Gulf of Alaska continental margin, *in* Scholl, D. W., Grantz, A., and Vedder, J. G., editors., Geology and resource potential of the continental margin of western North America and adjacent ocean basins—Beaufort Sea to Baja, California: Houston, Texas, Circum-Pacific Council for Energy and Mineral Resources, Earth Science Series, v. 6, p. 229–268.

Plafker, G., and Thatcher, W., 2008, Geological and geophysical evaluation of the mechanisms of the great 1899 Yakutat Bay Earthquakes, *in* Freymueller, J. T., Haeussler, P. J., Wesson, R. L., and Ekstrom, G., editors, Active tectonics and seismic potential of Alaska: American Geophysical Union Monograph, v. 179, p. 215–236.

Plafker, G., Jones, D., and Pessagno, E. A., Jr., 1977, A Cretaceous accretionary flysch and mélange terrane along the Gulf of Alaska margin, *in* Blean, K. M., editor, U.S. Geological Survey in Alaska: Accomplishments during 1976: USGS Circular 751-B, B41–B43.

Plafker, G., Hudson, T., Bruns, T. R., and Rubin, M., 1978, Late Quaternary offsets along the Fairweather Fault and crustal plate interactions in southern Alaska: Canadian Journal of Earth Sciences, v. 15, p. 805–816.

Plafker, G., Nokleberg, W. J., and Lull, J. S., 1989, Bedrock geology and tectonic evolution of the Wrangellia, Peninsular, and Chugach terranes along the Trans-Alaska Crustal Transect in the Chugach Mountains and southern Copper River Basin, Alaska: Journal of Geophysical Research, v. 94, n. B4, p. 4255–4295, doi:10.1029/JB094iB04p04255.

Plafker, G., Moore, J. C., and Winkler, G. R., 1994, Geology of the southern Alaska margin, *in* Plafker, G., and Berg, H. C., editors, The Geology of Alaska: Boulder, Colorado, Geological Society of America, Geology of North America, v. G-1, p. 389–449.

Rahn, M. K., Brandon, M. T., Batt, G. E., and Garver, J. I., 2004, A zero-damage model for fission-track annealing in zircon: American Mineralogist, v. 89, p. 473–484.

Raymo, M. E., 1994, The initiation of Northern Hemisphere glaciation: Annual Review of Earth and Planetary Sciences, v. 22, p. 353–383, doi:10.1146/annurev.ea.22.050194.002033.

Reiners, P. W., Spell, T. L., Nicolescu, S., and Zanetti, K. A., 2004, Zircon (U-Th)/He thermochronometry: He diffusion and comparison with $^{40}Ar/^{39}Ar$ dating: Geochimica et Cosmochimica Acta, v. 68, p. 1857–1887, doi:10.1016/j.gca.2003.10.021.

Richter, D. H., and Matson, N. A., Jr., 1971, Quaternary faulting in the Eastern Alaska Range: Geological Society of America Bulletin, v. 82, p. 1529–1539, doi:10.1130/0016-7606(1971)82[1529:QFITEA]2.0.CO;2.

Richter, D. H., Preller, C. C., Labay, K. A., and Shew, N. B., 2006, Geologic Map of the Wrangell-Saint Elias National Park and Preserve, Alaska: USGS Scientific Investigation Map 2877.

Ruppert, N. A., Ridgway, K. D., Freymueller, J. T., Cross, R. S., and Hansen, R. A., 2008, Active Tectonics of Interior Alaska: A synthesis of Seismic, GPS Geodesy, and Local Geomorphology, *in* Freymueller, J. T.,

Haeussler, P. J., Wesson, R. L., and Ekstrom, G., editors, Active Tectonics and Seismic Potential of Alaska: Geophysical Monograph Series, v. 179, p. 109–133.
Schuster, D. L., Flowers, R. M., and Farley, K. A., 2006, The influence of natural radiation damage on helium diffusion kinetics in apatite: Earth and Planetary Science Letters, v. 249, p. 148–161, doi:10.1016/j.epsl.2006.07.028.
Sisson, V. B., Poole, A. R., Harris, N. R., Burner, H. C., Pavlis, T. L., Copeland, P., Donelick, R. A., and McLelland, W. C., 2003, Geochemical and geochronologic constraints for genesis of a tonalite-trondjemite suite and associated mafic intrusive rocks in the eastern Chugach Mountains, Alaska: A record of ridge-transform subduction, *in* Sisson, V. B., Roeske, S. M., and Pavlis, T. L., editors, Geology of a transpressional orogen developed during ridge-trench interaction along the North Pacific margin: GSA Special Paper 371, p. 293–326, doi:10.1130/0-8137-2371-X.293.
Smith, W. H. F., and Sandwell, D. T., 1997, Global seafloor topography from satellite altimetry and ship depth soundings: Science, v. 277, p. 1956–1962, doi: 10.1126/science.277.5334.1956.
Spotila, J. A., Buscher, J. T., Meigs, A. J., and Reiners, P. W., 2004, Long-term glacial erosion of active mountain belts: Example of the Chugach-St. Elias Range, Alaska: Geology, v. 32, p. 501–504, doi:10.1130/G20343.1.
St. Amand, P., 1957, Geological and geophysical synthesis of the tectonics of portions of British Columbia, the Yukon Territory, and Alaska: The Geological Society of America Bulletin, v. 68, p. 1343–1370, doi:10.1130/0016-7606(1957)68[1343:GAGSOT]2.0.CO;2.
Stewart, R. J., Hallet, B., Zeitler, P. K., Malloy, M. A., Allen, C. M., and Trippett, D., 2008, Brahmaputra sediment flux dominated by highly localized rapid erosion from the easternmost Himalaya: Geology, v. 36, p. 711–714, doi:10.1130/G24890A.1.
Stock, J., and Molnar, P., 1988, Uncertainties and implications of the Late Cretaceous and Tertiary position of North America relative to the Farallon, Kula and Pacific plates: Tectonics, v. 7, p. 1339–1384, doi:10.1029/TC007i006p01339
Tagami, T., Galbraith, R. F., Yamada, R., and Laslett, G. M., 1998, Revised annealing kinetics of fission tracks in zircon and geological implications, *in* Van den haute, P., and De Corte, F., editors, Advances in Fission-Track Geochronolgy: Dordrecht, The Netherlands, Kluwer Academic Publisher p. 99–112.
Tomkin, J. H., 2007, Coupling glacial erosion and tectonics at active orogens: A numerical modeling study: Journal of Geophysical Research, v. 112, p. F02015, doi:10.1029/2005JF000332.
Tomkin, J. H., and Braun, J., 2002, The influence of alpine glaciation on the relief of tectonically active mountain belts: American Journal of Science, v. 302, p. 169–190, doi:10.2475/ajs.302.3.169.
Tomkin, J. H., and Roe, G. H., 2007, Climate and tectonic controls on glaciated critical-taper orogens: Earth and Planetary Science Letters, v. 262, p. 385–397, doi:10.1016/j.epsl.2007.07.040.
Trop, J. M., and Ridgway, K. D., 2007, Mesozoic and Cenozoic tectonic growth of southern Alaska: A sedimentary basin perspective, *in* Ridgway, K. D., Trop, J. M., Glen, J. M. G., and O'Neill, J. M., editors, Tectonic Growth of a Collisional Continental Margin: Crustal Evolution of Southern Alaska: Geological Society of America Special Paper, v. 431, p. 55–94, doi:10.1130/2007.2431(04).
Trop, J. M., Ridgway, K. D., Manuszak, J. D., and Layer, P., 2002, Mesozoic sedimentary-basin development on the allochthonous Wrangellia composite terrane, Wrangell Mountains basin, Alaska: A long-term record of terrane migration and arc construction: Geological Society of America Bulletin, v. 114, p. 693–717, doi: 10.1130/0016-7606(2002)114<0693:MSBDOT>2.0.CO;2
Trop, J. M., Ridgway, K. D., and Sweet, A. R., 2004, Stratigraphy, palynology, and provenance of the Colorado Creek basin, Alaska, U.S.A.: Oligocene transpressional tectonics along the central Denali fault system: Canadian Journal of Earth Sciences, v. 41, p. 457–480, doi:10.1139/e04-003.
Whipple, K. X., 2009, The influence of climate on the tectonic evolution of mountain belts: Nature Geoscience, v. 2, p. 97–104, doi:10.1038/ngeo413.
Whipple, K. X., and Meade, B. J., 2006, Orogen response to changes in climatic and tectonic forcing: Earth and Planetary Science Letters, v. 243, p. 218–228, doi:10.1016/j.epsl.2005.12.022.
Whipple, K., Kirby, E., and Brocklehurst, S. H., 1999, Geomorphic limits to climatically-induced increases in topographic relief: Nature, v. 401, p. 39–43, doi:10.1038/43375.
Willett, S., Beaumont, C., and Fullsack, P., 1993, Mechanical model for the tectonics of doubly vergent compressional orogens: Geology, v. 21, p. 371–374, doi:10.1130/0091-7613(1993)021<0371:MMFTTO>2.3.CO;2.
Witmer, J. W., Ridgway, K. D., Enkelmann, E., Brennan, P., and Valencia, V. A., 2009, Deposition, Provenance and Exhumation of Neogene Strata at the Syntaxis of the Chugach–St. Elias Range, southeast Alaska: GSA Annual Meeting, Portland, Abstract N. 108–25.
Yamada, R., Tagami, T., Nishimura, S., and Ito, H., 1995, Annealing kinetics of fission tracks in zircon: an experimental study: Chemical Geology, v. 122, p. 249–258, doi:10.1016/0009-2541(95)00006-8.
Zeitler, P. K., 2004, Arvert 4.0.1. Inversion of $^{40}Ar/^{39}Ar$ age spectra: User's Manual, http://www.ees.lehigh.edu/EESdocs/geochron/downloads/arvert401guide-US.pdf.
Zeitler, P. K., Koons, P. O., Bishop, M. P., Chamberlain, C. P., Craw, D., Edwards, M. A., Hamidullah, S., Jan, M. Q., Khan, M. A., Khattak, M. U. K., Kidd, W. S. F., Mackie, R. L., Meltzer, A. S., Park, S. K., Pecher, A., Poage, M. A. Sarker, G., Schneider, D. A., Seeber, L., and Shroder, J. F., 2001, Crustal reworking at Nanga Parbat, Pakistan: Metamorphic consequences of thermal-mechanical coupling facilitated by erosion: Tectonics, v. 20, p. 712–728, doi:10.1029/2000TC001243.
Zweck, C., Freymueller, J. T., and Cohen, S. C., 2002, Three-dimensional elastic dislocation modeling of the postseismic response to the 1964 Alaska earthquake: Journal of Geophysical Research, v. 107, B4, 2064, doi:10.1029/2001JB000409.